Université Mohamed Khider de Biskra
Entrez votre faculté
Entrez votre département

MÉMOIRE DE MASTER

Domaine : Sciences et Techniques
Filière : Génie Mécanique
Spécialité : Energétique

Réf. : Entrez la référence du document

Présenté et soutenu par :
M. Islem Benzaf

Le : mercredi 11 juin 2024

conception d'un dispositif météorologique avec création d'un modèle mathématique pour prédire les paramètres environnementaux

---

Jury :

M.	Adnane Labed	Pr	Université de Biskra	Président
M.	Foued Chabane	Pr	Université de Biskra	Rapporteur
M.	Hefaidh Hadef	MCA	Université de Biskra	Examinateur

Année universitaire : 2023 - 2024

Mohamed Khider University of Biskra
Enter your faculty
Enter your department

MASTER MEMORY

Field: Science and Technology Sector: Mechanical Engineering Specialty: Energy

Ref. : Enter the document reference

Presented and supported by:
Mr. Islem Benzaf
On: Wednesday 11 June, 2024

design of a meteorological device with creation of a mathematical model to predict environmental parameters

---

Jury :

M.	Adnane Labed	Pr	University of Biskra	President
M.	Foued Chabane	Pr	University of Biskra	Rapporteur
M.	Hefaidh Hadef	MCA	University of Biskra	Examiner

College year: 2023 - 2024

Thanks

I would like to extend my sincere thanks to Allah, the big thank you goes to him, for my help and the will he gave to overcome all the obstacles and difficulties during my years of study and for having enlightened my path in order to achieve this modest

work.

I would like to thank my supervisor: Prof. Foued Chabane for agreeing to supervise this dissertation, for the advice he gave me and for the efforts he made throughout the completion of this work.

I thank Pr. Adnane labed
for agreeing to chair the jury.

I thank Dr. Hefaidh HADEF for agreeing to examine this dissertation and being a member of the jury.

I would like to express my sincere thanks to my parents, my family

and any person who participated from far or near in the outcome of this

modest work.

Islam benzaf

Dedications

I dedicate my work to those who gave me life:

my dad and mom

All my siblings: Soumia, Sarah, Fodil, Diaa. Nour Dine, Aya, Najib.

My friends: Ossama, Alaa, Fateh, Fares, Hamza, Doudo, Marwan

All my friends and acquaintances, without exception.

Everyone who helped and encouraged me.

All mechanical power engineering upgrade.

Islambenzaf

Résumé

Ce travail vise à développer un modèle mathématique pour prédire le rayonnement solaire global en utilisant un ensemble de variables météorologiques telles que la température, la pression atmosphérique et l'angle d'élévation solaire. Les résultats expérimentaux ont montré un accord significatif entre le modèle mathématique et les données expérimentales, confirmant sa précision dans la prédiction du rayonnement solaire. Un dispositif de mesure a été conçu en utilisant la plateforme Arduino et des capteurs précis pour mesurer de manière continue et fiable les variables météorologiques. Ce modèle peut être appliqué pour améliorer la conception et le fonctionnement des systèmes d'énergie solaire et améliorer leur efficacité. Ce document ouvre des perspectives pour des développements futurs, notamment l'ajout de nouvelles variables pouvant affecter le rayonnement solaire et l'amélioration de la précision des capteurs utilisés, favorisant ainsi l'utilisation durable et efficace de l'énergie renouvelable.

Summary

This work aims to develop a mathematical model for predicting global solar radiation using a set of meteorological variables such as temperature, atmospheric pressure, and solar elevation angle. Experimental results showed significant agreement between the mathematical model and experimental data, confirming its accuracy in solar radiation prediction. A measurement device was designed using the Arduino platform and precise sensors to continuously and reliably measure meteorological variables. This model can be applied to improve the design and operation of solar energy systems and enhance their efficiency. The paper opens avenues for future developments including the addition of new variables that may affect solar radiation and improving the accuracy of the sensors used, thus promoting the sustainable and effective utilization of renewable energy.

ملخص

تهدف هذه المذكرة إلى تطوير نموذج رياضي للتنبؤ بالإشعاع الشمسي العالمي باستخدام مجموعة من المتغيرات الجوية مثل درجة الحرارة، والضغط الجوي، وزاوية ارتفاع الشمس. أظهرت النتائج التجريبية توافقًا كبيرًا بين النموذج رياضي والبيانات التجريبية، مما يؤكد دقته في التنبؤ بالإشعاع الشمسي. تم تصميم جهاز قياس يعتمد على منصة الأردوينو وحساسات دقيقة لقياس المتغيرات الجوية، وأثبت فعاليته في جمع البيانات بشكل مستمر وموثوق. يمكن تطبيق هذا النموذج لتحسين تصميم وتشغيل أنظمة الطاقة الشمسية وزيادة كفاءتها. تفتح هذه المذكرة آفاقًا لتطويرات مستقبلية تشمل إضافة متغيرات جديدة قد تؤثر على الإشعاع الشمسي وتحسين دقة الحساسات المستخدمة، مما يعزز من استغلال الطاقة المتجددة بشكل مستدام وفعّال.

Content

CHAPTER I Bibliographic study

CHAPTER II Devices and their connection

Chapter III Experimental and theoretical study

Chapter IV Results and discussion

Chapter I

Chapter II

Chapter III

Chapter IV

Chpter I

Chpter II

Chpter III

Nomenclature

φ: Latitude of the location (°)

δ: The declination of the sun (°)

P: atmospheric pressure (atm)

G: the monthly average daily global radiation over a horizontal surface (W/m^2)

G0: monthly average daily extraterrestrial radiation on a horizontal surface a horizontal surface (W/m^2)

L : longitude (°)

w: The hour angle (°)

TSV: True solar time (heur)

MST: Mean Solar Time (heur)

TU: Universal time (heur)

TL: Legal time (heur)

I2C : Inter-Integrated Circuit, wiring type

VCC : The positive pole of the direct voltage

GND : (Ground) the negative pole of the direct voltage

SDA : SerialDATA (serial data)

SCL : Serial Clock

LCD : Liquid Crystal Diode (this is a display device)

AO : Analogue Output

DO : Digital Output

AVR : (Automatic Voltage Regulator) voltage regulator, this term is used by Atmel to designate the core of the processor and the family of microcontrollers which implement it

PIC : (Programmable Interface Controller), programmable controller

TX : Transmitter

RX : Receiver

IDE : Integrated Development Environment

General introduction

General introduction

The Sun, as a vital source of energy, is essential for life on Earth. The global solar radiation that the Sun reaches us is a key indicator of the distribution of solar energy and its impacts on the environment and climate. Among the regions that are characterized by great importance in the study of solar radiation is the Biskra region in Algeria.

The Biskra region is characterized by its distinctive geographical and climatic conditions that make it an ideal place for conducting experiments and scientific studies related to solar radiation. Biskra has rich, constant year-round solar radiation, as well as mild winter and hot summer temperatures, making it an ideal location to study the effects of solar radiation on the environment and climate.

From this standpoint, Biskra is considered an ideal destination for conducting experiments and scientific studies aimed at understanding the relationship between weather conditions, solar radiation, and its effects on the environment and climate. This memorandum will take advantage of Biskra's suitable and distinctive environment to achieve its goals of studying global solar radiation and analyzing its effects more accurately and comprehensively.

This experiment aims to create a device for measuring and predicting weather conditions based on a complex mathematical equation that takes into account several variables of weather conditions such as temperature, humidity, wind speed, atmospheric pressure, lighting intensity, and the percentage of ultraviolet radiation. This aims to provide a deeper and more accurate understanding of the effects of solar radiation on the environment and climate, by analyzing the relationship between weather factors and amounts of solar radiation.

This study consists of four chapters

1. Chapter One Bibliographic Studies: In this chapter, we will review previous studies related to global solar radiation and its effects on the environment and climate. We will review the main findings and conclusions and analyze them in more detail.
2. Chapter Two Devices and their connection: In this chapter, we will review the devices and technologies used to measure global solar radiation, including platforms such as Arduino and appropriate sensors. We will explain how to connect and program it appropriately.
3. Third chapter Experimental and theoretical study: In this chapter, we will carry out an experimental and theoretical study to analyze the effects of different weather conditions on

global solar radiation. We will develop a measuring device and create a mathematical equation linking weather conditions and solar radiation.

4. Chapter Four Results and conclusion: In this chapter, we will present the results of the measurements and analyses obtained, and we will analyze them in depth. We will discuss trends, changes, and variations in global solar radiation based on weather conditions.

CHAPTER I

I.1 Introduction:

Understanding the impact of solar radiation and thermal radiation on the environment and climate is fundamental for many environmental and technological applications. Numerous previous studies have been conducted to understand how radiation is affected by various parameters. Meteorological Researchers have examined various aspects of this subject, including:

1. Cloud Impact on Radiation: Previous studies have shown that clouds play a crucial role in distributing radiation on the Earth's surface. Clouds are capable of converting direct solar radiation into scattered radiation, affecting temperatures and weather patterns.

2. Climate Impact of Solar Storms: Previous studies have demonstrated that solar storms can affect the Earth's atmosphere, leading to changes in solar radiation and atmospheric activities.

3. Climate Impact on Thermal Radiation: Thermal radiation emitted from the Earth's surface is significantly influenced by factors such as air temperature, humidity, and soil type. Many studies have been conducted to understand these relationships.

4 Climate Change and Radiation: Scientists seek to understand how climate change, such as rising temperatures and changes in humidity levels, affects the distribution of radiation and weather patterns.

These previous studies contribute to expanding our knowledge of the impact of weather conditions on radiation and how they affect the environment and climate. They provide an important framework for understanding environmental and climatic changes in the future.

I.2 Bibliographic study

The aims study focuses on creating a model that illustrates the prediction curve of global solar radiation according to some weather parameters, in this part of the chapter we can present the report's study depending on our study:

A comprehensive study in Yazd, Iran, aimed to estimate global solar radiation using various mathematical models. Performance evaluation metrics such as RMSE, MBE, MABE, MPE, and correlation coefficient (r) were employed. Among the models tested, the El-Metwally model exhibited superior performance in estimating global solar radiation on a horizontal surface in Yazd and similar climatic regions. The mathematical models utilized

included the El-Metwally model, Badescu model, Hargreaves model, and Chen et al. model. Monthly average global solar radiation estimates were generated for Yazd, with the El-Metwally model proving most accurate and effective for this purpose. [1]

The report details the development of a model to forecast global solar radiation, considering factors such as ambient temperature, location, date, and time. This modeling aids in understanding how these variables impact solar radiation for solar energy conversion. Model accuracy was evaluated by comparing predictions with experimental measurements at the Biskra site, showing good agreement. Comparison with existing models, like M-Y Mechraoui and M. Capderoui's, provided a comprehensive assessment of accuracy. Small errors between measured and calculated values suggest reliability in estimating global solar radiation levels under similar conditions. Overall, the study provides valuable insights into accurately predicting global solar radiation, offering a benchmark for future research. [2]

The object of the reported work is the presentation of an approach for the estimate of global irradiation, by clear sky and average sky, applicable to the whole of the Algerian territory. An approach that takes account of the nature of the Algerian network of measurements, characterized by a low density of radiometric stations (7 stations) distributed on a surface of approximately 2 500 000 km². The application of the analysis in principal components to the fraction of insolation measured by 54 stations of the network of the National Office of Meteorology made it possible to define five energy zones homogeneous. A relation of the Angström type connecting the monthly global solar irradiation to the fraction of insolation was established for each zone. Its extrapolation to the whole of the network is presented in the form of charts. The radiation by the clear sky is modeled, for five radiometric stations, according to the zenith distance illustrating the distribution on a large scale of monthly global irradiation. [3]

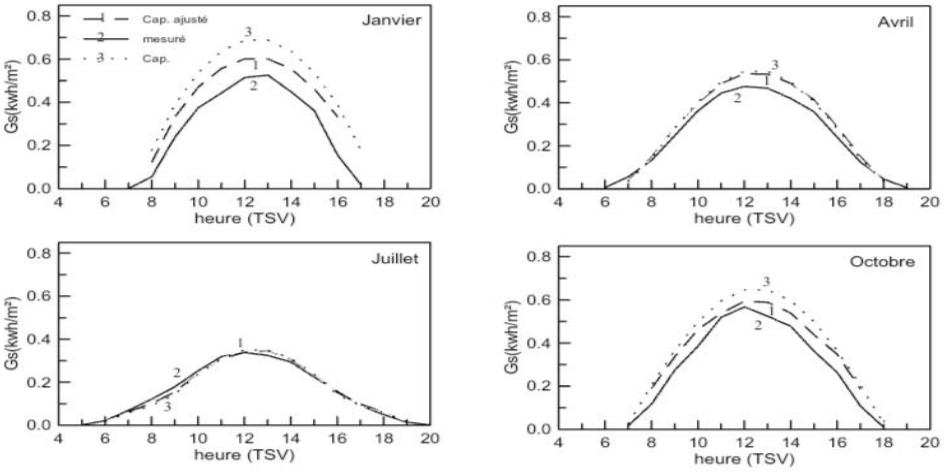

Fig.I.1 The normal direct irradiance under clear sky measured and simulated by the Cap and adjusted Cap models

The research report focuses on developing a method to estimate monthly average solar irradiance on tilted surfaces using only monthly average sunshine duration as input. The aim is to provide a practical tool for designing and implementing solar energy systems across different regions of Morocco. Detailed calculations were conducted for various locations, including Rabat, to validate the method by comparing estimated irradiance values with actual measurements. Beyond technical advancements, the research aims to support socio-economic development and environmental sustainability in Morocco, particularly in enhancing rural electrification programs through better utilization of solar energy resources. Overall, the study offers a valuable contribution to optimizing solar energy system design and implementation in Moroccan settings by leveraging easily accessible weather data like sunshine duration measurements. [4]

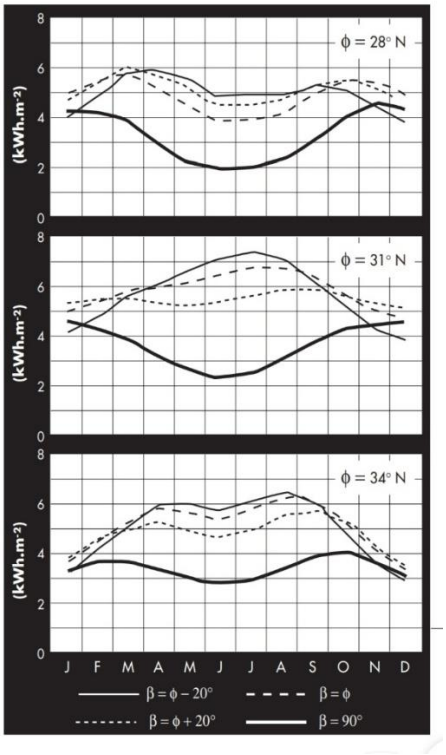

Fig.I.2 Estimation of the monthly average daily global solar irradiation on an inclined plane for three Moroccan latitudes.

The report study aimed to address the lack of solar radiation data and predictive models in Algeria's Big South region by developing and readjusting models to estimate daily and monthly mean global solar irradiation. These models utilized ground data of air temperature, sunshine hours, and day/month numbers. Evaluation using the K-fold cross-validation method revealed that only sunshine-based models provided excellent estimations at a daily scale, with validation RMSEs ranging from 1.470 to 2.425 MJ/m² day. Additionally, all developed models demonstrated superior performance in estimating monthly mean global irradiation levels, with relative root mean square errors (RRMSE) mostly below 10%. This underscores the importance of accurate solar resource predictions for designing and evaluating solar energy projects in Algeria's desert climate. The study emphasized the significance of the K-fold 1cross-validation method in optimizing error estimates and stabilizing model performances, aiding in selecting appropriate models for accurate solar irradiation estimation under Algerian desert conditions. [5]

The objective of the study is to predict global solar radiation (GSR) on the horizontal surface in Relizane, Algeria, using an artificial neural network (ANN). The optimal ANN model, trained and tested with 80% and 20% of the data, respectively, yielded the best results with a 10-25-1 structure (10 inputs, 25 hidden, and 1 output neurons).

During the test stage, the model showed excellent agreement with experimental data, achieving a correlation coefficient (R) of 0.9879, root mean squared error (RMSE) of 47.7192 (Wh/m^2), mean absolute error (MAE) of 27.7397 (Wh/m^2), and mean squared error (MSE) of 2.2771e+03 (Wh/m^2). The model utilized a three-layer Feedforward neural network with a Regularization Bayesienne (trainer) training algorithm, employing hyperbolic tangent sigmoid and linear transfer functions at the hidden and output layers, respectively. The results demonstrate accurate predictions with an RMSE of less than 0.50 (Wh/m^2) and an R-value exceeding 0.98, indicating high acceptability. This ANN model can be valuable for designing solar energy systems in hot regions. [6]

	Training phase	Training phase	Total phase
R	0.9872	0.9879	0.9873
MAE (wh/m^2)	27.8925	27.7397	27.8619
RMSE (wh/m^2)	48.6154	47.7192	48.4375
SEP (%)	21.4145	20.9351	21.3188
RER (wh/m^2)	21.4246	21.7716	21.5033
RPD (wh/m^2)	6.2715	6.4435	6.3051
MSE (wh/m^2)	2.3635e+03	2.2771e+03	2.3462e+03
MRSE (wh/m^2)	2.6865e-04	3.5958e-04	2.8597e-04
REA (wh/m^2)	0.0164	0.0190	0.0169
AF (wh/m^2)	1.0001	1.0081	1.0017

BF (wh/m²)	1.0001	1.0081	1.0017

Table.I.1 Statistical Evaluation of the Models Performance

A comprehensive study was conducted to estimate global solar radiation in Yazd, Iran, using several mathematical models. The performance of these models was evaluated using mathematical metrics such as RMSE, MBE, MABE, MPE, and correlation coefficient (r). The results showed that the El-Metwally model provides the best estimation of global solar radiation on a horizontal surface in Yazd and similar climatic regions

These models were used to estimate the monthly average global solar radiation on a horizontal surface in Yazd, and the results demonstrated the accuracy and effectiveness of the El-Metwally model in this context.[7]

The study aims to model global solar radiation in Algeria using geographical and climatic parameters like sunshine duration, temperature, and humidity. Statistical regression techniques were applied to develop models for estimating daily solar radiation on a horizontal plane, tested on two Algerian sites from 2001-2005. Results emphasize the importance of air temperature and relative humidity in accurately predicting solar radiation. Using only temperature and humidity variables sufficiently modeled solar radiation, achieving regression values between 72.30% and 91.00%. The research offers valuable insights for designing photovoltaic systems based on accurate solar energy predictions in Algeria. [8]

The report focuses on predicting global hourly solar irradiation for the Adrar region in Algeria, where solar radiation data are limited, crucial for supporting renewable energy projects. Data from Adrar's Saharan Renewable Energy Research Unit and the SODA database spanning six years (2013-2018) were utilized. Nine models with three activation functions were tested, utilizing input parameters related to solar geometry and astronomical data. A neural model with a logistic Sigmoid activation function and 15 neurons in the hidden layer demonstrated exceptional performance, achieving a correlation coefficient of 98.25% between measured and estimated global solar irradiation. This suggests the model's effectiveness not

only for Adrar but potentially for similar climatic regions. Leveraging artificial intelligence, this study developed a robust model crucial for optimizing renewable energy projects by accurately predicting hourly global solar irradiance values. [9]

This article aims to propose a methodology to reconstruct monthly average hourly reflected and total solar radiation based on monthly averages of solar radiation throughout the day for some atmospheric parameters. In this research, several theoretical or experimental models were studied that link the monthly averages of both reflected and total solar radiation to some meteorological and astronomical variables. These models were used to compare the measured values with the estimated values, and the results were presented in tables showing the relative error and standard deviation values for each model and each month of the year. It was concluded that some models provided good results in estimating total and reflected solar radiation, while some models showed overestimations or inaccurate estimates. [10]

The study aimed to develop a model for predicting global solar radiation on inclined surfaces at the Biskra site in Algeria. Experimental data from pyranometer measurements were used to propose an exponential model, which was compared with established ones like Perrin de Brichambaut's. The proposed model accurately estimated solar radiation, with coefficients such as tilt factor and azimuth angle playing vital roles. The research emphasized the importance of precise solar radiation prediction for solar energy conversion. Another study focused on predicting global solar irradiation at different tilt angles in Ouled Djellal, Algeria, using parameters like solar declination and hour angle. The developed site-specific model was validated against experimental results, showing reliability for forecasting solar irradiation levels crucial for optimizing solar energy systems. [11]

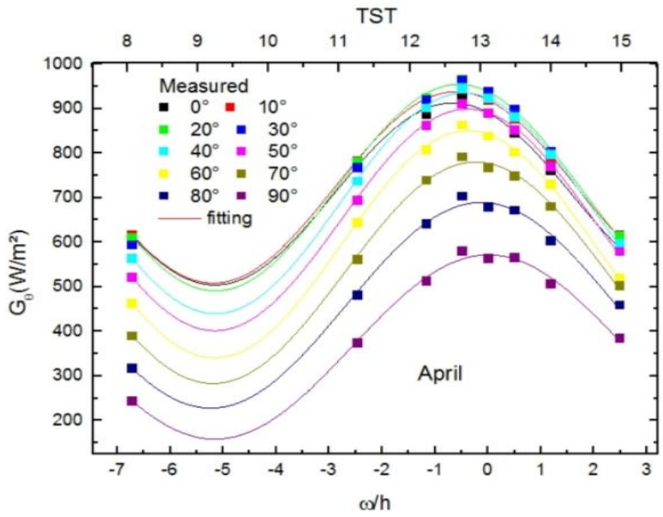

Fig.I.3 Comparison of global irradiation according to tilt angles between Model and experimental data in April

The report compares empirical models from existing literature with newly developed models for estimating global solar radiation on a horizontal surface in Muğla, Turkey. Meteorological data collected from 2007 to 2015 using a Kipp and Zonen pyranometer at Muğla Sıtkı Koçman University are analyzed. A total of 105 literature models are evaluated using MATLAB, employing statistical tests including MBE, MPE, MAPE, MABE, RMSE, and R^2. Only two models (Veeran and Kumar/model 24, Chegaar and Chibani/model 35) meet the acceptable ± 10% statistical error limits. Seven new models are developed, achieving error values below 0.8 and high R^2 values. Data sets are divided into two semesters (January – June and July – December) to improve model accuracy. Additionally, Benson's model is examined and compared with previous ones, concluding that cubic and quadratic models are suitable for January – June and July – December periods, respectively. [12]

The study employed two models to estimate the monthly average daily global solar radiation on horizontal surfaces in Algeria. The first model, adapted from Barbaro et al.'s formula, was calibrated for Algerian locations using the equation:

$$R=a+b\cdot H+c\cdot\sin(\phi)\cdot\sin(\delta)+d\cdot\cos(\phi)\cdot\cos(\delta)\cdot\cos(H) \quad (I.1)$$

where R is the global solar radiation, H is the solar hour angle, ϕ is the latitude of the location, and δ is the solar declination angle. The second model utilized a linear regression equation of the Angstrom type:

$$R=a+b\cdot n \quad (I.2)$$

where R is the global solar radiation, n is the sunshine duration, and a and b are regression coefficients. Data from four meteorological stations were analyzed, showing both models provided accurate estimates compared to measured data. Specific zone parameters were determined for each location. Maximum absolute errors ranged from 7-10%, indicating strong agreement between measured and estimated values. Overall, the study highlighted the effectiveness of these models in estimating global solar radiation across diverse Algerian climates. [13]

The report study aimed to compare two models for calculating solar radiation in Algeria: the Capderou model, commonly used but criticized for inaccuracies, and the r.sun model, a newer alternative. The research focused on measuring solar radiation values at two sites in Algeria (Bouzaréah and Ghardaïa) and comparing them with estimates from these models. Results showed that the r.sun model provided better estimations of direct and diffuse components of solar radiation with low relative errors compared to the Capderou model. The study highlighted how accurate estimation of solar radiation is crucial for designing efficient solar energy systems. Additionally, it was noted that while both models had their strengths and weaknesses, overall r.sun outperformed Capderou in providing more reliable estimations.

In conclusion, the research emphasized the importance of using advanced modeling techniques like r.sun over traditional methods like Capderou when estimating solar radiation data for designing effective renewable energy systems in regions like Algeria.[14]

Erreur relative moyenne journalière (%)		Horizontal						Incliné	
		R. diffus		R. direct		R. global		R. global	
		ASA	r.sun	ASA	r.sun	ASA	r.sun	ASA	r.sun
Bouza Réah	14/01/06	7.48	50.77	26.07	5.63	18.22	11.43	36.83	24.71
	14/03/06	23.05	67.76	6.23	1.78	7.57	5.71	15.51	12.07
	09/07/06	35.73	61.40	3.79	2.15	5.23	4.45	4.15	2.41
	18/11/06	40.98	81.08	16.04	9.15	18.98	17.94	33.70	31.48
Ghardaïa	22/01/08	23.05	67.76	6.23	1.78	7.57	5.71	15.51	12.07
	04/03/08	35.73	61.40	3.79	2.15	5.23	4.45	4.15	2.41
	12/06/08	40.98	81.08	16.04	9.15	18.98	17.94	33.70	31.48
	15/10/08	52.02	25.17	26.28	7.26	2.81	2.43	12.32	5.05

Table.I.2 Calculation results of relative errors of horizontal solar radiation and inclined for a few clear days, on the two chosen sites

This study aimed to develop theoretical models for estimating the total solar radiation received at the Earth's surface, considering the effects of reflection and absorption that solar radiation undergoes as it passes through the atmosphere. These models were based on determining the transmission coefficients of various atmospheric components, requiring current weather conditions and geographical information for the site. Models from Lacis & Hansen, Bird & Hulstrom, Atwater & Ball, and Davies & Hay were simulated for sites in Ghardaïa and Bouzaréah in Algeria.

The comparative study of the results obtained showed that the Davies & Hay and Bird & Hulstrom models provide a better estimation of solar radiation, with negligible errors between measured and calculated values. In conclusion, these semi-empirical models for solar radiation demonstrated their ability to compare measured values with estimated ones, confirming that there is no universal theoretical approach to estimating solar radiation, and that integration between approaches based on direct measurements and those estimated from satellite imagery is necessary. [15]

I.2 Conclusion

Understanding the interplay between radiation and meteorological parameters is essential for comprehending climate dynamics. The studies reviewed emphasize the significant influence of factors like cloud cover, solar storms, and climate variations on radiation distribution. Moving forward, continued research in this area will be vital for effective environmental management and climate adaptation strategies.

CHAPTER II

II.1. Introduction

The Arduino platform is indeed renowned for its versatility, catering to both hobbyists and professionals alike, facilitating the creation and programming of diverse electronic systems. These systems heavily leverage a plethora of sensors to measure an array of phenomena including temperature, light, and humidity. These sensors are seamlessly integrated with Arduino devices through tailored input/output interfaces, empowering users to seamlessly decipher and leverage data for the development of an array of applications. In this chapter, we embark on a journey to explore the devices employed, the intricacies of connecting them, and the nuanced art of programming them.

II.2. Defining sensors

A sensor is a device that converts an observed physical measurement into an electrical measurement, which is then translated into binary data that can be used and understood by an information system. Sensors record various types of measurements such as temperature, humidity, light, acceleration, sound, and more. The concept of sensors has evolved, with their application areas expanding. Initially, sensors were dedicated to measuring only one type of measurement, but modern sensors represent a combination of multiple devices capable of measuring various physical phenomena. [9]

II.2.1 Description of the Arduino MEGA Board

The Arduino Mega 2560 is based on the Atmega2560 microcontroller, which is more powerful compared to Uno and Nano, allowing the board to handle more complex projects that require power and speed in computation [16].

II.2.1.1Power Supply

The Arduino Mega 2560 board can be powered either via a USB connection (providing 5V up to 500mA) or using an external power supply. The power source is automatically selected by the board. The board can operate with an external power supply of 6 to 20 volts.

II.2.1.2 Visualization

There is an LED included on the board connected to the small pin 13 for hardware testing with a microcontroller connection. The other LEDs are used to indicate transmission and reception during program downloading into the microcontroller.

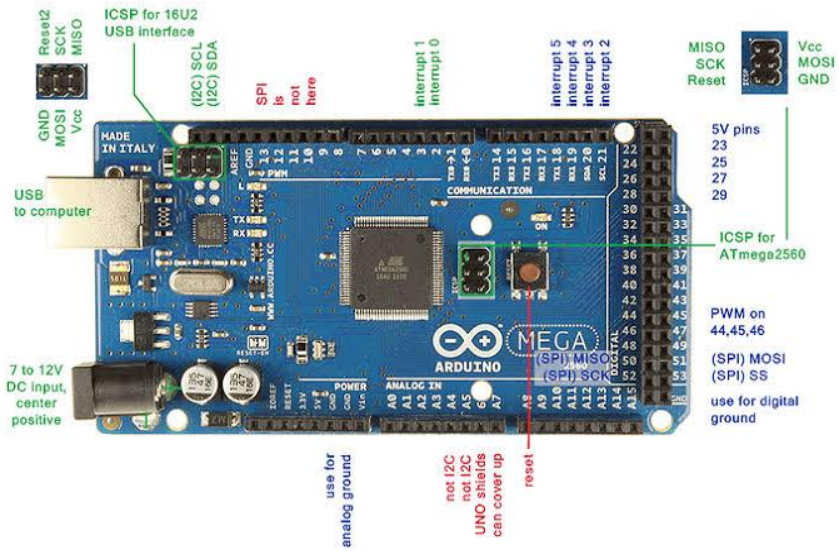

Fig II.1 Description of the Arduino MEGA 2560 board.[17]

II.2.2. The temperature sensor and humidity sensor (DHT11)

DHT11 is a digital temperature and humidity sensor. This sensor contains a calibrated digital signal output. The sensor comprises resistive components sensitive to moisture and a temperature measurement device. It is connected to a high-performance 8-bit microcontroller. The DHT11 sensor is capable of measuring temperatures from 0 to +50°C with an accuracy of +/- 2°C and relative humidity levels from 20 to 80% with an accuracy of +/- 5%. A measurement can be taken every second.[18].

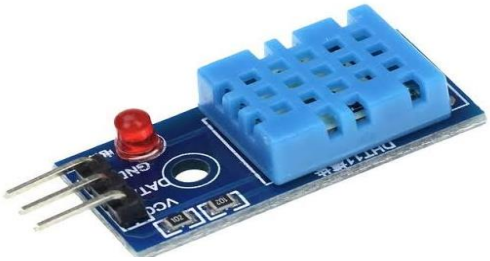

Fig II.2 Temperature and humidity sensor (DHT11).

II.2.3 Pressure sensor(BMP180)

The BMP180 is an integrated circuit developed by Bosch Sensoriel. It is designed specifically to measure atmospheric pressure. Typically, it is used for weather observations and for determining altitude from pressure. The integrated circuit is very small and does not require additional components to measure barometric pressure, altitude, and temperature.

II.2.3.1 Main characteristics of the pressure sensor (BMP180)

Les caractéristiques de ce capteur sont [19] :

- Tension d'alimentation: 3.3V DC
- Interface: I2C (jusqu'à 3,4 MHz), SPI (jusqu'{ 10 MHz
- Température: -40 à + 85 ° C
- Humidité: 0-100%
- Pression: 300-1100 hpa

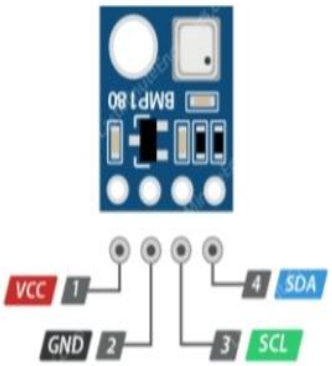

Fig II.3 pressure sensor(BMP180)

II.2.4 Soil moisture sensor

The Soil Moisture Sensor is used to measure the volumetric water content of soil. This makes it ideal for performing experiments in courses such as soil science, agricultural science, environmental science, horticulture, botany, and biology.[20]

II.2.4.1 Features

Operating Voltage: 3.3V – 5V

•Small Size – 1.6cm*3cm

•Dual Output Mode

•Adjustable Sensitivity with Dash Built-in Potentiometer Power Indicator (Red LED) and Digital Output Indicator (Green LED)

Fig II.4 Soil moisture sensor

II.2.5 Sensor MQ-135

The MQ135 is a sensor for measuring air quality. The MQ135 is sensitive to the main pollutants present in the atmosphere of the house. This sensor is sensitive to CO2, alcohol, benzene, nitrogen oxide (Nox), and ammonia (NH3).[21]

II.2.5.1 FEATURES

- Rated voltage: 5V
- 2 Outputs: Analog and digital on or off according to an adjustable threshold
- The module has an LED indicator of the status of the digital output
- Detects NH3, Nox, alcohol, benzene, smoke, and CO_2
- High sensitivity: 10 – 300 ppm NH3, 10 – 1000 ppm Benzene, 10 – 300 Alcohol
- The higher the concentration, the higher the analog output

Fig II.5 MQ-135 Sensor

II.2.6 BH1750FVI sensor

BH1750FVI sensor module is an optical digital IC interface density digital light sensor with two serial bus wires. Using the data collection light intensity can be set from the stiffness of the Backlightclavierdel. The decision unit allows detect a wide range of light intensity.

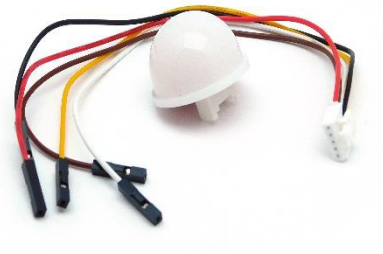

Fig II.6 BH 1750 FVI Sensor

II.2.7 Voltage sensor

25V voltage detection sensor module, This is a simple but very useful module that uses a potential divider to reduce an input voltage by a factor of 5. The 25V voltage sensor module allows you to use the analog input of a microcontroller to monitor voltages much higher than it is capable of detecting.[22]

Fig II.7 Voltage sensor

II.2.8 Ultra Violet Sensor

The UV sensor is used to detect the intensity of incident ultraviolet (UV) radiation. This form of electromagnetic radiation has shorter wavelengths than visible. The UV sensor is based on the GUVA-S12D sensor which has a wide spectral range of 200nm-400nm. The electrical signal output module varies with the intensity of the UV radiation [23]

Fig II.8 Sensor ultraviolet

II.2.9 Micro SD Card

Micro SD Card Module Supports Micro SD Card, Micro SDHC card (high-speed card). The level conversion circuit board that can interface level is 5V or 3.3V. The communication interface is a standard SPI interface control Interface: A total of six pins (GND, VCC, MISO, MOSI, SCK, CS), GND to ground, VCC is the power supply, MISO, MOSI, SCK is the SPI bus, CS is the chip select signal pin; 3.3V regulator circuit: LDO regulator output 3.3V as level converter chip, Micro SD card supply.MicroSD card toward the direction of the control interface MISO signal is also converted to 3.3V, general AVR microcontroller system can read the signal.[24]

Fig II.9 Micro SD Card

II.3 Arduino Software

II.3.1 Overview IDE

Arduino IDE (Integrated Development Environment) is a software for Arduino. It is used to write code, compile code for debugging, and upload code to Arduino. It is a cross-platform software available on all operating systems such as Windows, Linux, and macOS. It is open-source software that allows users to use the software as they please. You can also create your modules/functions and add them to the software.[25]

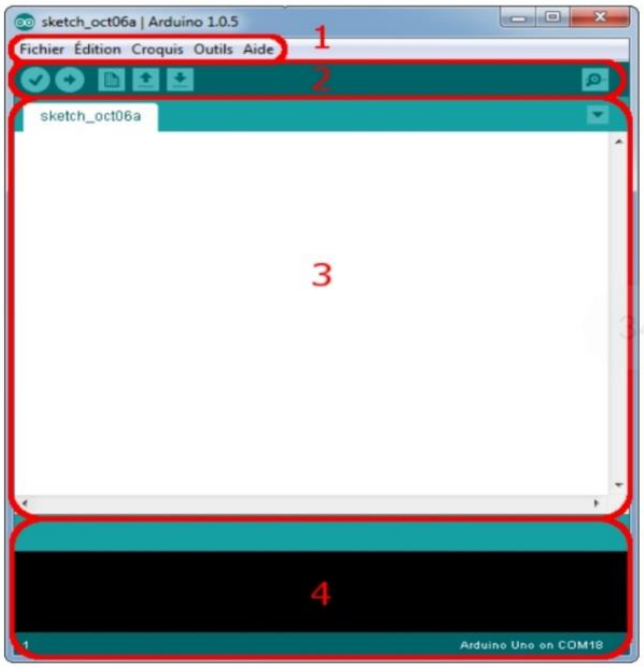

Fig II.10 The Arduino Program Interface

- Frame number 1: These are the configuration options of the software
- Frame number 2: Contains the buttons used when programming the card
- Frame number 3: This block contains the program to create
- Frame number 4: This is important because it helps to fix errors in the program. This is a debugger.

- The keys of the Arduino IDE interface

Fig II.11 The Keys of the Arduino IDE interface

The following table briefly represents the functions of each button[25].

key 1	This button allows you to check the program, it activates a module that looks for errors in your program
Key 2	Loads (uploads) the program into the Arduino board
Key 3	Creates a new file
Key 4	Open a file
Key 5	Saves the file.
Key 6	Open the serial monitor (we'll see what it is later).

Table II.1 Key of the Arduino IDE interface

II.3.2 Language of the Arduino

Arduino programming language is very similar to C ++, which is a popular language in the computer world. The code you learn to write an Arduino is very similar to the code you write in other computer languages. The basic concepts are all the same. In reality, you have just learned to use another dialect [26]

II.4 Connection and programming

II.4.1 Sensor DHT 11

To connect the DHT11 sensor to an Arduino:

1. Connect the VCC pin to 5V on the Arduino.

2. Connect the GND pin to any GND pin on the Arduino.

3. Connect the Signal pin to a digital pin on the Arduino (e.g., Digital Pin 2).

After the connection, you can use the DHT11 library in Arduino to read temperature and humidity values from the sensor.

Fig II.12 Assembly of DHT11 real photo

Once the device is connected and the Arduino board is powered, we can program it to read data from the DHT11 sensor.

```
#include <dht11.h>
#define DHT11PIN 4
dht11 DHT11;
void  setup()
{
Serial.begin(9600);
}
void loop()
{
Serial.println();
int chk = DHT11.read(DHT11PIN);
Serial.print("Humidity (%): ");
Serial.println((float)DHT11.humidity, 2);
Serial.print("Temperature  (C): ");
Serial.println((float)DHT11.temperature, 2);
delay(2000);
}
```

Fig II.13 Programming DH11 sensor [27]

II.4.2 Soil humidity sensor

To connect a soil moisture sensor to an Arduino:

1. Connect the VCC (power) wire from the sensor to the 5V pin on the Arduino.

2. Connect the GND (ground) wire from the sensor to any GND pin on the Arduino.

3. Connect the Signal wire from the sensor to an analog input pin on the Arduino, such as Analog Pin A0.

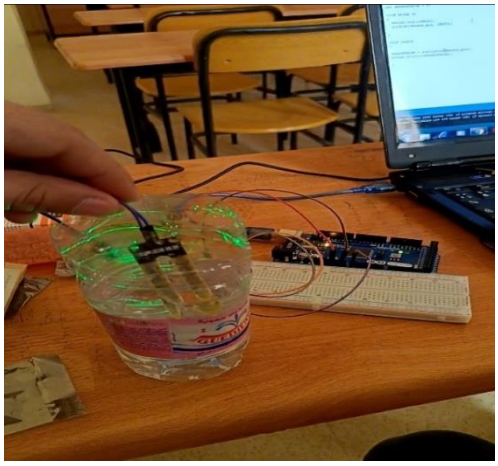

Fig II.14 Assembly of real photo soil moisture sensor.

After connecting, you can use the Arduino software to read the values from the soil moisture sensor

```
// Moisture Sensor Arduino Code
//By Circuitdigest
#define ledPin 6
#define sensorPin A0
void setup() {
Serial.begin(9600);
pinMode(ledPin, OUTPUT);
digitalWrite(ledPin, LOW);
}
void loop() {
Serial.print("Analog output: ");
Serial.println(readSensor());
delay(500);
}
//  This function returns the analog data to calling function
int readSensor() {
int sensorValue = analogRead(sensorPin);  // Read the analog value from sensor
```

```
int outputValue = map(sensorValue, 0, 1023, 255, 0); // map the 10-bit data to 8-bit data
analogWrite(ledPin, outputValue); // generate PWM signal
return outputValue;           // Return analog moisture value
}
```

Fig II.15 Programming Soil Moisture Sensor [28]

II.4.3 Sensor MQ 135

connect the MQ-135 gas sensor to an Arduino board:

1. Connect the VCC pin of the sensor to the 5V pin on the Arduino.

2. Connect the GND pin of the sensor to any GND pin on the Arduino.

3. Connect the Digital Out pin of the sensor to a digital pin on the Arduino (such as Digital Pin 2).

4. Connect the Analog Out pin of the sensor to an analog input pin on the Arduino (such as Analog Pin A0).

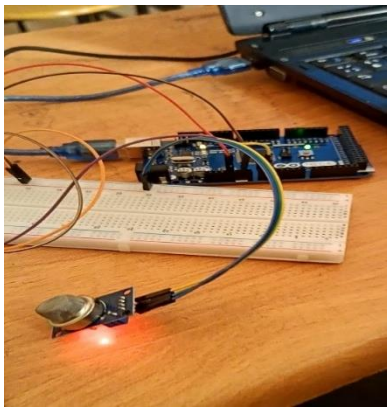

Fig II.16 Assembly of MQ 135 Sensor actual photo

After connecting, you can program the Arduino to read sensor data and take appropriate actions accordingly.

```
Void setup() {
  Serial.begin(9600);
}
Void loop() {
  Int sensorValue = analogRead(A0);
```

```
  Serial.println("The amount of CO2 (in PPM): ");
  Serial.println(sensorValue);
  Delay(2000);
}
```

Fig II.17 Programming Sensor MQ 135 [29]

II.4.4 BH1750FVI light sensor

To connect the BH1750FVI light sensor to Arduino:

1. Connect VCC to Arduino's 5V.

2. Connect GND to any GND pin on Arduino.

3. Connect SDA to Arduino's SDA pin.

4. Connect SCL to Arduino's SCL pin.

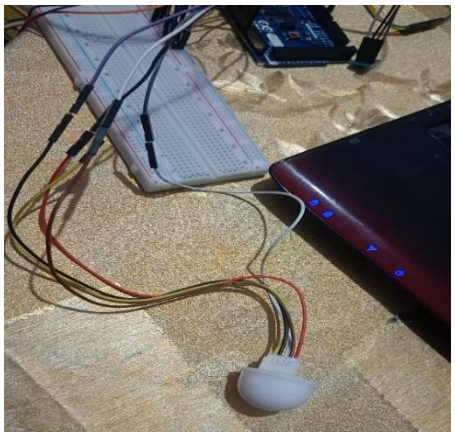

Fig II.18 BH1750FVI assembly real photo

After connection,you can use the Arduino software to read the values from the BH1750FVI light sensor

```
#include <Wire.h>
#include <BH1750.h>
BH1750 lightMeter;
void setup() {
  Serial.begin(9600);
  lightMeter.begin();
}
```

```
void loop() {
  uint16_t lux = lightMeter.readLightLevel();
  Serial.print("Lux: ");
  Serial.println(lux);
  // Convert lux to W/m²
  float watts_per_square_meter = lux * 0.0079; // Adjust this value according to the appropriate relationship
  Serial.print("W/m^2: ");
  Serial.println(watts_per_square_meter);
  delay(1000);
}
```

Fig II.19 Programming BH1750FVI light sensor [30]

II.4.5 BMP180 Sensor

To connect the BMP180 pressure sensor to Arduino:

1. Connect VCC to Arduino's 5V.

2. Connect GND to any GND pin on Arduino.

3. Connect SDA to Arduino's SDA pin.

4. Connect SCL to Arduino's SCL pin.

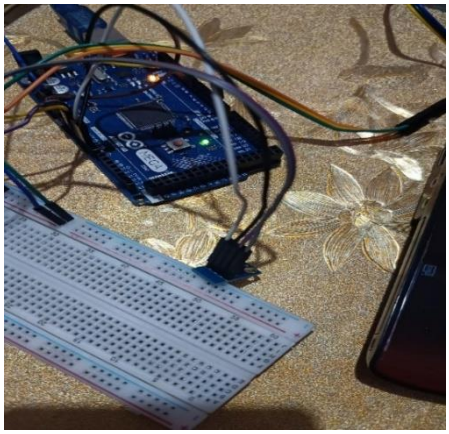

Fig II.20 Assembly of BMP180 Sensor Real Photo

After the connection, you can use the Arduino software to read the values from the temperature data from the sensor.

```
#include <Wire.h>
```

```
#include <Adafruit_BMP085.h>
Adafruit_BMP085 bmp;
void setup() {
Serial.begin(9600);
if (!bmp.begin()) {
Serial.println("Could not find BMP180 or BMP085 sensor.");
while (1) {}
}
void loop() {
Serial.print("Pressure: ");
float pressure_hPa = bmp.readPressure() / 100.0; // Convert pressure from Pa to hPa
Serial.print(pressure_hPa);
Serial.println(" hPa");
delay(1000);
}
```

Fig II.21 Programming Sensor bmp 180 [31]

II.4.6 Voltage sensor

To connect a voltage sensor to an Arduino board briefly:

1. Connect the ground (GND) of the sensor to the ground (GND) on the Arduino board.

2. Connect the positive terminal (-) of the sensor to one of the analog input pins on the *Arduino* board.

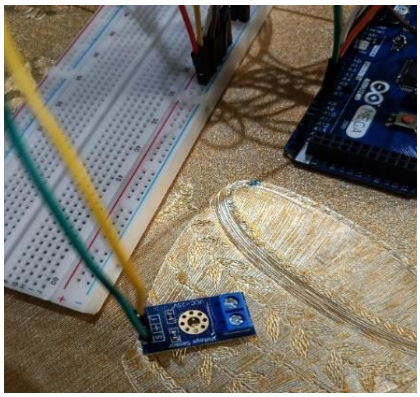

Fig II.22 Voltage sensor

Program the Arduino to read the voltage value from the analog input pin connected to the sensor.

```
// Define the analog pin to which the voltage sensor is connected
const int voltageSensorPin = A0;
// Variables to store sensor readings and calculated speeds
float measuredVoltage = 0.0;
float measuredSpeedOfFan = 0.0;
float speedAnemometer = 0.0;
void setup() {
  // Initialize serial communication for debugging
  Serial.begin(9600);
}
void loop() {
  // Read the analog value from the voltage sensor
  int sensorValue = analogRead(voltageSensorPin);

  // Convert the analog value to voltage (assuming a 5V reference)
  measuredVoltage = sensorValue * (5.0 / 1023.0);
  // Convert the voltage to fan speed (example conversion factor)
  // This conversion factor should be determined based on your specific sensor and fan setup
  measuredSpeedOfFan = measuredVoltage * 2.0; // Placeholder conversion factor
  // Calculate the anemometer speed using the derived equation
  speedAnemometer = 4.08 * measuredSpeedOfFan - 0.278;
  // Print the results to the serial monitor for debugging
  Serial.print("Measured Voltage: ");
  Serial.print(measuredVoltage);
  Serial.print(" V, ");
  Serial.print("Fan Speed: ");
  Serial.print(measuredSpeedOfFan);
  Serial.print(" m/s, ");
  Serial.print("Anemometer Speed: ");
  Serial.println(speedAnemometer);
  // Add a delay for stability
  delay(1000);
}
```

Fig II.23 Voltage Sensor Programming

II.4.7 Ultraviolet (UV) sensor

1. Connect the VCC pin of the sensor to the 5V input on the Arduino.

2. Connect the GND pin of the sensor to the GND input on the Arduino.

3. Connect the signal output pin of the sensor to an Analog Input pin on the Arduino.

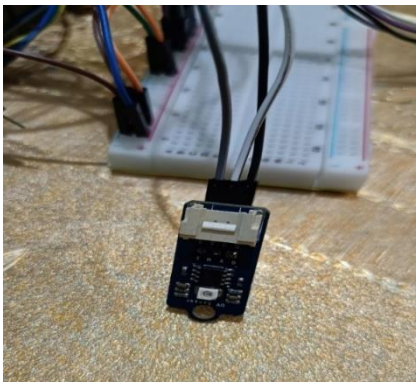

Fig II.24 Assembly of Ultraviolet (UV) sensor in the real photo

Program the Arduino to read the appropriate value from the Analog Input pin.

```
// Define the output pin
Const int outputPin = A0;
// Conversion factor from reading to watts per square meter
Const float conversionFactor = 5.0 / 1024.0; // Based on the operating voltage of the sensor
Void setup() {
  // Set up the pin from which the signal from the sensor is read
  pinMode(outputPin, INPUT);
  // Start serial communication with the computer
  Serial.begin(9600);
}
Void loop() {
  // Read the value from the sensor
  Int sensorValue = analogRead(outputPin);
  // Convert the value to watts per square meter
 Float uvIntensity = sensorValue * conversionFactor;
  // Print the value to the serial port
  Serial.print("UV intensity (W/m^2): ");
  Serial.println(uvIntensity, 4); // Print the value with 4 decimal places
```

```
  // Wait for one second before reading the next value
  Delay(1000);
}
```

Fig II.25 Programming Ultraviolet (UV) sensor [32]

II.5 Conclusion

In this chapter, we have given a brief description of different sensors used for the realization of our weather station. Thus, a presentation of the Arduino board was made giving all the technical details of the latter.

CHAPTER III

III.1 Introduction

Weather monitoring and forecasting are vital for daily decision-making and safety. This chapter explores the construction of a simple weather monitoring device to enhance understanding of local weather phenomena. We will focus on key elements and offer practical guidance for creating such a device. Through this process, readers will gain insight into meteorology and learn how to effectively handle data quality challenges.

III.2 Experimental study

III.2.1 Site of the experimental setup

Figure III.1 shows the local place for examining our study, which is next to the hall technology at the University of Biskra, we can determine this site by latitude and longitude coordinate φ = 34.845364° and L = 5.747029, respectively.

Fig III.1 Experimental setup

III.2.2 Climate of the site of Biskra

The results of the measurement data have takes correspond to the website Infoclimat [33], which gives different results of the ambient temperature, pressure, and wind speed with direction. In this part of the results, we have taken the days corresponding to our work on the airport of the Biskra. The discussion of some cures in the days of 05/05/2024, 06/05/2024, 07/05/2024, and 08/05/2024.

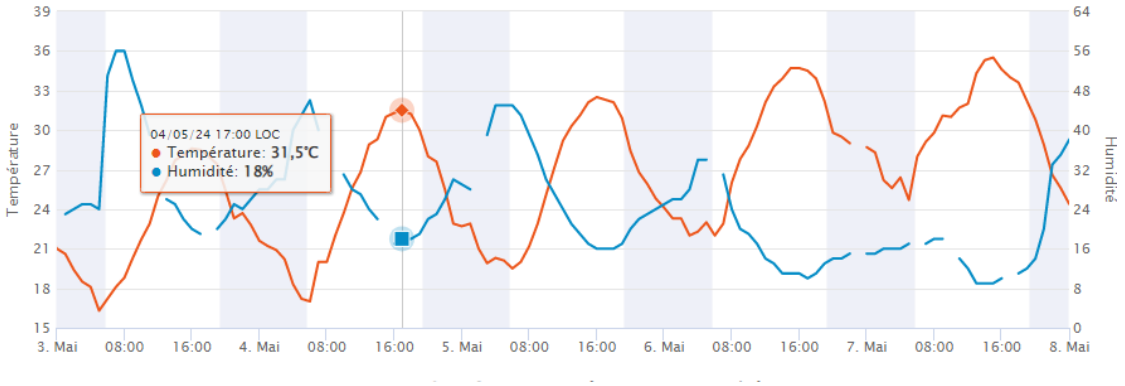

Fig.III.2 Evolution of the ambient temperature corresponding to the site of the airport of the Biskra

Figure III.2 represents the variation of ambient temperature as a function of the time of the day. We can see that the variation of the curves takes the sinusoidal form function which depends on the sunrise and sunset of the solar radiation which gives us a minimal value of the temperature and the height value represents the value of the midday when the solar radiation takes a higher value.

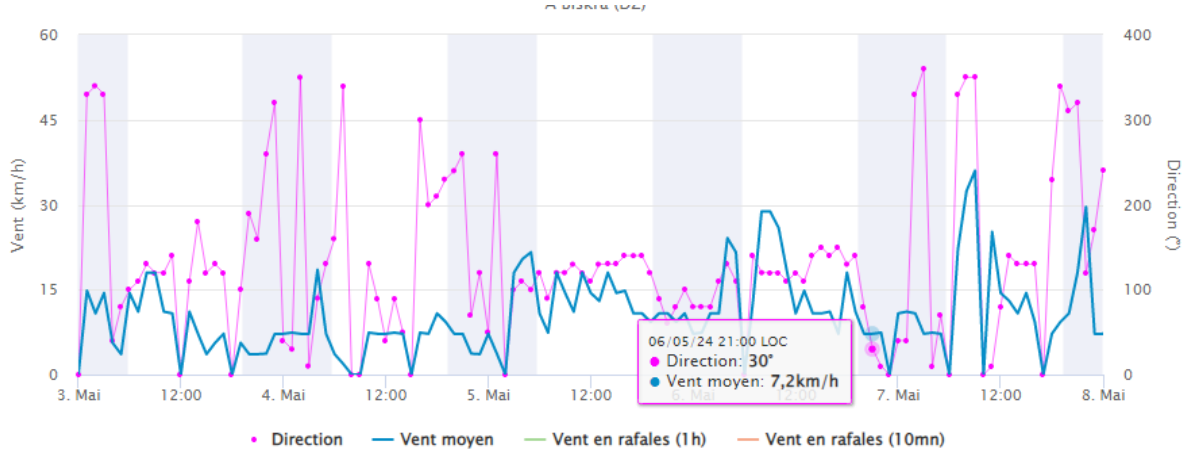

Fig.III.3 Evolution of the wind speed with direction corresponding to the site of the airport of the Biskra

Figure III.3 shows the variation of the wind speed and direction as a function of the time of the day. We can observe that the variation of the wind speed is not regular evolution and this part has affected the results of the solar collector, estimated in the lost heat of the collector and the drying room.

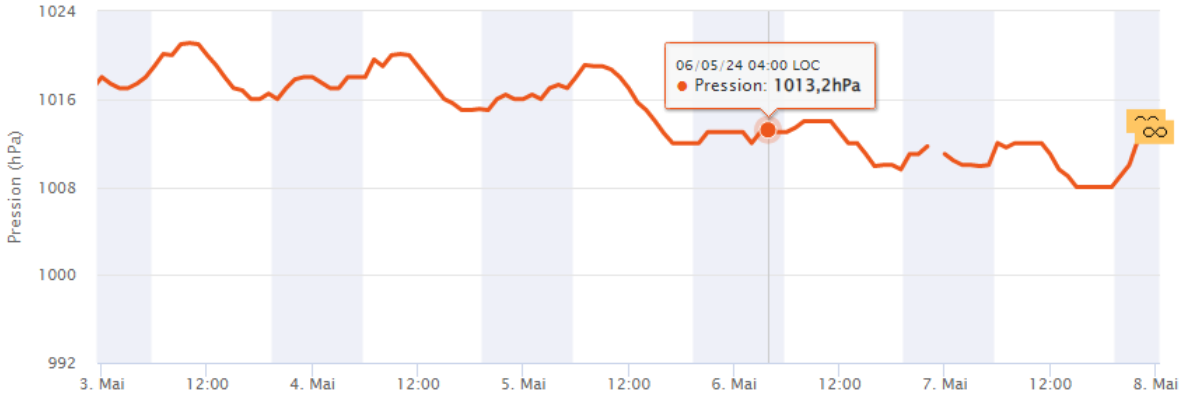

Fig.III.4 Evolution of the pressure corresponding to the site of the airport of the Biskra

Figure III.4 shows the variation of the pressure as a function of the time of the day from 03/05/2024 to 08/05/2024. The curve of the pressure has irregular evolution caused by the variation of the air temperature according to the weather of the day.

III.2.3 Manufacturing a Weather Device: Steps and Details

III.2.3.1 Manufacturing the Device:

To manufacture the weather device, a sequence of steps is required to ensure its assembly correctly and effectively.

III.2.3.2 Preparing the Box:

The process starts with preparing the device's box, where a suitable box with dimensions of 40x25x25 cm is chosen, and a door is installed on it using hinges to allow easy access inside. The box is also equipped with insulation to provide additional protection for the internal devices.

Fig III.5 Measurement day box

III.2.3.3 Installing LCD I2C Screens:

Next, multiple LCD screens are installed inside the door using I2C connectors, a technology that allows connecting several screens without the need for many wires, to display weather measurement data directly and in an easily readable format.

Fig III.6 Front end of a box

III.2.3.4 Preparing Arduino, Breadboard, and Sensor Installation:

In this step, the Arduino Mega board is prepared inside the box alongside the breadboard. Additionally, atmospheric sensors are installed above the device, including temperature and humidity sensor (DHT11), air quality sensor (MQ135), light intensity sensor (BH1750FVI), barometric pressure sensor (BMP180), and ultraviolet sensor (UV). The soil moisture sensor (Soil Moisture Sensor) is placed on the side for connection to the soil. These configurations ensure efficient data collection and monitoring of weather conditions and soil moisture levels effectively.

Fig.III.7 Measurement day box

III.2.3.5 Connecting Sensors to Arduino:

The sensor wires are connected to the correct ports on the breadboard and then to the Arduino Mega, where the Arduino is programmed to read data from the sensors accurately and respond immediately.

Fig III.8 Box inside

III.2.3.6 Arduino Programming:

After that, the Arduino is programmed to analyze the measured data and display it in an organized manner on the LCD screens, and to perform any additional functions such as recording data or sending it over the Internet for remote environmental monitoring.

III.2.3.7 Testing the Device:

After assembling the device completely, a comprehensive test is conducted to ensure that all parts work correctly and display data accurately and reliably on the LCD screens.

III.2.4 Instruments devices

Our experimental study needs some instrument devices for measuring some parameters such as solar radiation, wind speed, temperature, weight, and humidity. All instrument devices have names according to the measured parameter.

III.2.4.1 Digital anemometer

The digital anemometer helps us to measure the wind speed and the mass flow rate, see Fig.III.9.

Fig III.9 Digital anemometer

III.2.4.2 Hygrometer

The hygrometer is an important device used to help us measure the humidity and ambient temperature outside of the experimental setup, see Fig.III.10.

Fig III.10 Hygrometer

III.2.4.3 Pyranometer

This device is important for measuring the global solar radiation under a tilt angle equal to 38°, which measures every 30 minutes in the day starting at 9h00 to 16h00, see Fig.III.11.

Fig III.11 Pyranometer

III.2.4.4 Lux Meter

A Lux Meter is a device used to measure the intensity of illumination (luminous flux) in a given environment, expressing the results in units of "lux" to enable the assessment and adjustment of lighting levels for optimal conditions.

Fig III.12 Lux Meter

III.2.Measuring wind speed

To measure wind speed, we connected an 8 cm diameter computer fan to a voltage sensor to convert the resulting voltage into speed. The fan was exposed to airflow at different rates using an airflow generator, and we compared the results obtained with an anemometer under the same conditions.

Fig III.13 Aspirator

The following table shows these comparisons:

Airflow ratio(%)	Measured Fan Speed (m/s)	Anemometer Wind Speed (m/s)
24	0.4	1.48
30	0.82	3
40	1.22	4.8
50	1.52	6
60	1.81	6.8
70	2	7.5

Table III.1 Determination of the corresponding speed fan by instrument of anemometer

To convert the measured fan speed values to equivalent values from the anemometer, a linear equation derived from the experimental data can be used:

$$\text{Speed anemometer} = 4.08 \times \text{Speed fan} - 0.278 \quad \text{(III.1)}$$

Then we can add this equation to the Arduino programming.

III.3 Theoretical study

III.3.1 Global solar radiation

Solar radiation, also known as solar resource, is electromagnetic radiation emitted by the sun that can be converted into energy through various technologies, depending on the available solar resource.

III.3.2 Basic Principles

Every location on Earth receives sunlight for at least part of the year. The amount of solar radiation that reaches any one spot on the Earth's surface varies according to:

- Geographic location
- Time of day
- Season
- Local landscape
- Local weather.

III.3.3 Diffuse and direct solar radiation

As sunlight passes through the atmosphere, some of it is absorbed, scattered, and reflected by:

- Air molecules
- Water vapor
- Clouds
- Dust
- Pollutants
- Forest fires
- Volcanoes.

Global solar radiation combines diffuse and direct radiation, with atmospheric conditions reducing direct beam radiation by 10% on clear days and 100% on thick days.

$$Globalsolarradiation = Directr\ radiation + Diffuse\ radiation \quad \text{(III.2)}$$

III.3.4 Declination of the sun δ

The solar declination is the angle formed by the normal to the elliptical plane and the axis of rotation of the earth. It can also be defined as the angle between the center line of the sun center of the earth and its projection on the equatorial plane of the earth. Its expression is given by:

$$\delta = 23{,}45 \sin [0{,}980(j + 284)] \quad \text{(III.3)}$$

III.3.5 Azimuth a:

It is the horizontal angle measured from the meridian, positively towards the west and negatively towards the east, allowing locating the position of the sun. The azimuth is 0 ° when it crosses the meridian of a place. The relationship of the azimuth is as follows:

$$\text{Sin (a)} = \frac{\sin(w)\cos\delta}{\cosh}$$

$$\Rightarrow a = \arcsin\left[\frac{\sin w.\cos\delta}{\cosh}\right] \quad \text{(III.4)}$$

With:

ω: Time angle

δ : Declination of the sun

h: height of the sun

III.3.6 Height of the sun h:

The Height angle (used interchangeably with altitude angle) is the angular height of the sun in the sky measured from the horizontal. Confusingly, both altitude and elevation are also used to describe the height in meters above sea level. The elevation is 0° at sunrise and 90° when the sun is directly overhead (which occurs for example at the equator on the spring and fall equinoxes).

The expression of h is as follows:

$$\sinh = \sin\delta\sin\varphi + \cos\delta\cos\varphi\cos\omega \quad \Rightarrow h = \arcsin\left[\sin\delta\sin\varphi + \cos\delta\cos\varphi\cos\omega\right] \text{ (III.5)}$$

with: φ : Longitude of place

III.3.7 Latitude:

It is the angle formed between the vertical of a place and the plane of the equator. The latitudes are positive to the north and negative to the south.

III.3.8 Longitude φ :

Longitude of a place: Angle that forms the meridian of a place with the meridian of origin of Greenwich. The longitude is counted positively towards the west and negatively towards the east.

- Longitude deviation: the time difference between the meridian of a place and a reference meridian (Greenwich or the time zone). There is an offset of 4 minutes per degree of longitude.

III.3.9 Hour angle ω :

is the angular displacement of the sun east or west of the local meridian due to rotation of the earth on its axis at 15°per hour; morning negative afternoon positive (solar time must be in hours, hour angle in degrees):

$$\omega = \frac{360}{24} \text{ (TST- 12)} \qquad \text{(III.6)}$$

With: TST: true solar time.

III.3.10 Angle of incidence θ :

The angle of incidence is the angle formed between the direct solar radiation and the normal to the sensor inclined concerning the horizontal plane by an angle i (see figure III.14). For a sensor oriented towards the south, Incidence can be deduced:

$$\cos\theta = \cos(\varphi - i)\cos\delta\cos\omega + \sin(\varphi - i)\sin\delta \qquad \text{(III.7)}$$

If the capture is not oriented south θ can be found from h, α analytically:

$$\cos\theta = \cosh\cos(a - \gamma)\sin i + \sinh\cos i$$

0(III.8)

In winter i = φ +10° ;

In summer i = φ -10°

i represent the angle of inclination and γ The orientation concerning the direction of the south.

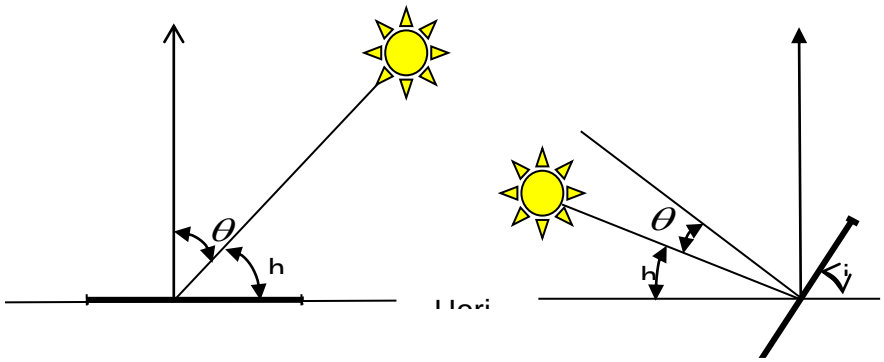

Horizontal Tilt capture

Fig.III.14 Representations of the angle of incidence θ

III.3.11 Mathematical model of the Global solar radiation

The purpose of this part of the study is to create an established model for forecasting the evolution of Global solar radiation. Trying to choose the perfect equation to agree with the trajectory of the experiment points of the test, can be observed that a good function represented by the Logistic function, which is found in the OriginLab version 8 helps us to give our model.

a. Boltzmann Function

The Boltzmann function represents a good model for predicting form of the Global solar radiation, the established model has four constants such as a, b, c; and d, and these constants are affected by month and weather parameters, we can observe that all constants had effected by some parameters such as the type of which estimated the month and days, when the global solar radiation as a function to h

$$G_H(h,T,Tr,P,nbrM) = a + \frac{(b-a)}{\left(1+\exp\left(\frac{\left[\left(\frac{T}{P}\right)^{\frac{nbrM}{10}\times h} + \left(\frac{Tr}{T}\right)\times\sin(h)\right] - c}{d}\right)\right)} \quad \text{(III.8)}$$

The relationship started with putting the independent variable x see eq. (III.9) which depending the different parameters of the climate such as ambient temperature, dew temperature, pressure, and the number of months without forgetting the height of the sun angle. We can propose a relationship of x by the new formula, see eq. (III.9).

$$x = \left(\frac{T}{P}\right)^{\frac{nbrM}{10}\times h} + \left(\frac{Tr}{T}\right)\times\sin(h) \quad \text{(III.9)}$$

The dependent variable is estimated as the global solar radiation see eq. (III.10).

$$y = G_H \quad \text{(III.10)}$$

We found that a good illustration curve is by the Logistic function in the OriginLab, which is shown in equation III.11.

$$y = a + \frac{(b-a)}{1+\exp\left(\frac{x-c}{d}\right)} \quad \text{(III.11)}$$

Table III.2 shows the constants a, b, c, and d of the forecast model which are determined according to month. About the global solar radiation calculated by important constants

Month	January	February	March	April
B	-4.48251	-3.73111	-15.58009	-2.88189
A	686.5889	781.72161	930.37581	1039.25322

C	0.30101	0.27821	0.28826	0.33412
D	0.12099	0.09825	0.12071	0.0934
R^2	0.95603	0.96624	0.98355	0.98767

Table III.2 The constants of the prediction model for each month

III.4 Conclusion

This chapter presents an experimental and theoretical study aimed at developing a mathematical model to predict global solar radiation ratios based on climatic parameters such as pressure, temperature, and relative humidity. A theoretical study can only be considered valid if it is supported by experimental data. The experimental aspect relies on using measurement instruments as reference tools to obtain accurate values. Additionally, we have detailed the process of constructing the measurement device.

CHAPTER IV

IV.1 Introduction

Within this chapter, we will present the results of meteorological measurements collected and analyzed over a specific period, focusing on graphical curves illustrating changes in climatic elements such as temperature, humidity, atmospheric pressure, and wind speed, along with global solar radiation. The data will be systematically presented and analyzed using statistical methods, with the results interpreted and linked to known meteorological phenomena. This chapter aims to provide a comprehensive view of weather changes, enhancing scientific understanding of climatic conditions and their practical applications across various fields. Measurements were taken from the beginning of January to the end of April, conducted at Biskra Airport.

IV.2 Ambient, and dew temperature

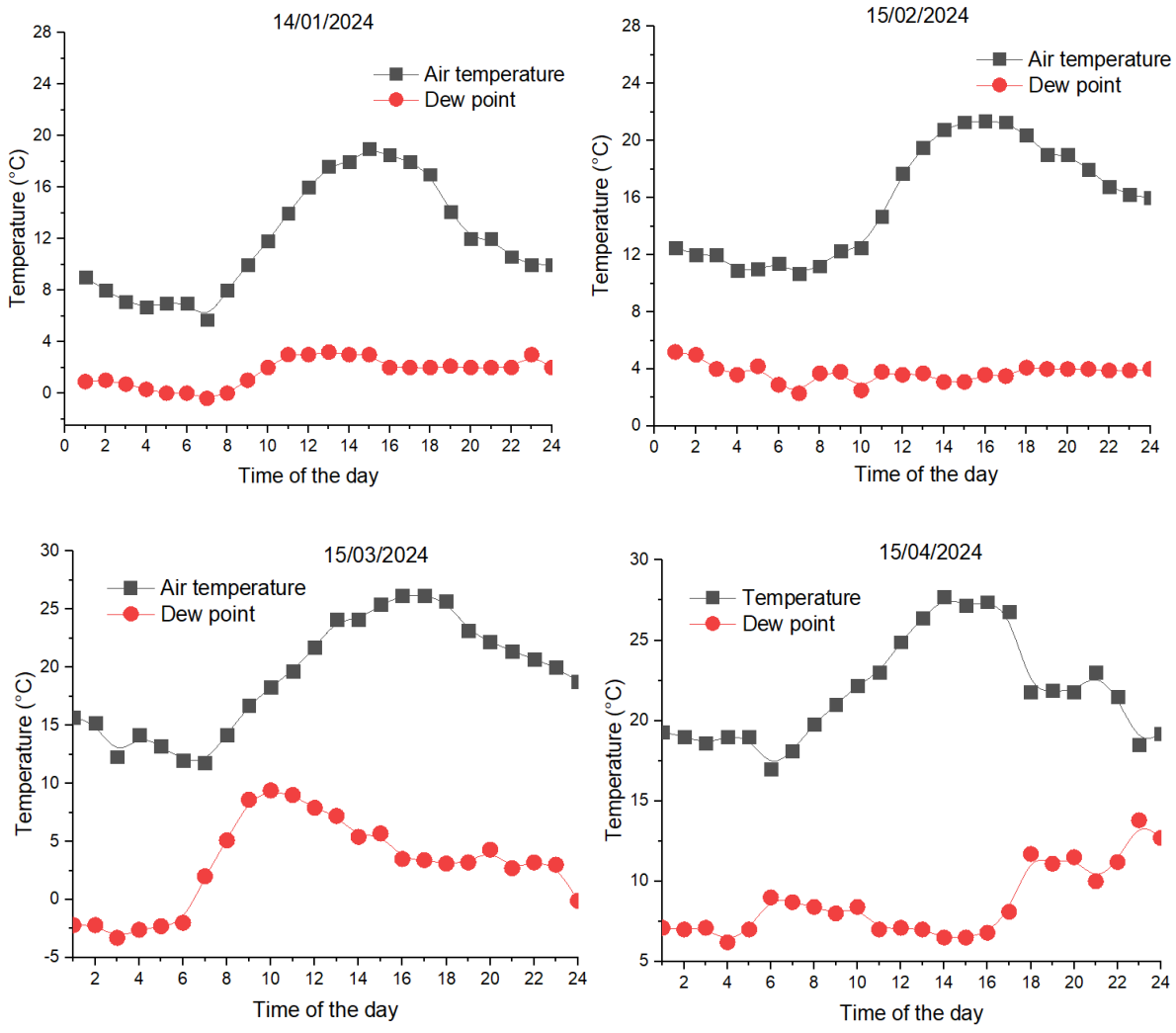

Fig.IV.1 Ambient, and dew temperature versus time of the day.

The data obtained from the experiment conducted in Biskra shows periodic changes in ambient temperature and temperature of dew point throughout the day see Fig.IV.1. There is a noticeable rise in temperature during daylight hours and a decrease after sunset, which reflects the significant impact of solar radiation. Similarly, the dew point follows a similar pattern on the date 14/01/2024 against other dates, sometimes the dew temperature takes the same evolution with ambient temperature, and sometimes not. These results are important for understanding atmospheric processes in the region and their impact on the surrounding environment.

IV.3 Humidity relative to site of Biskra

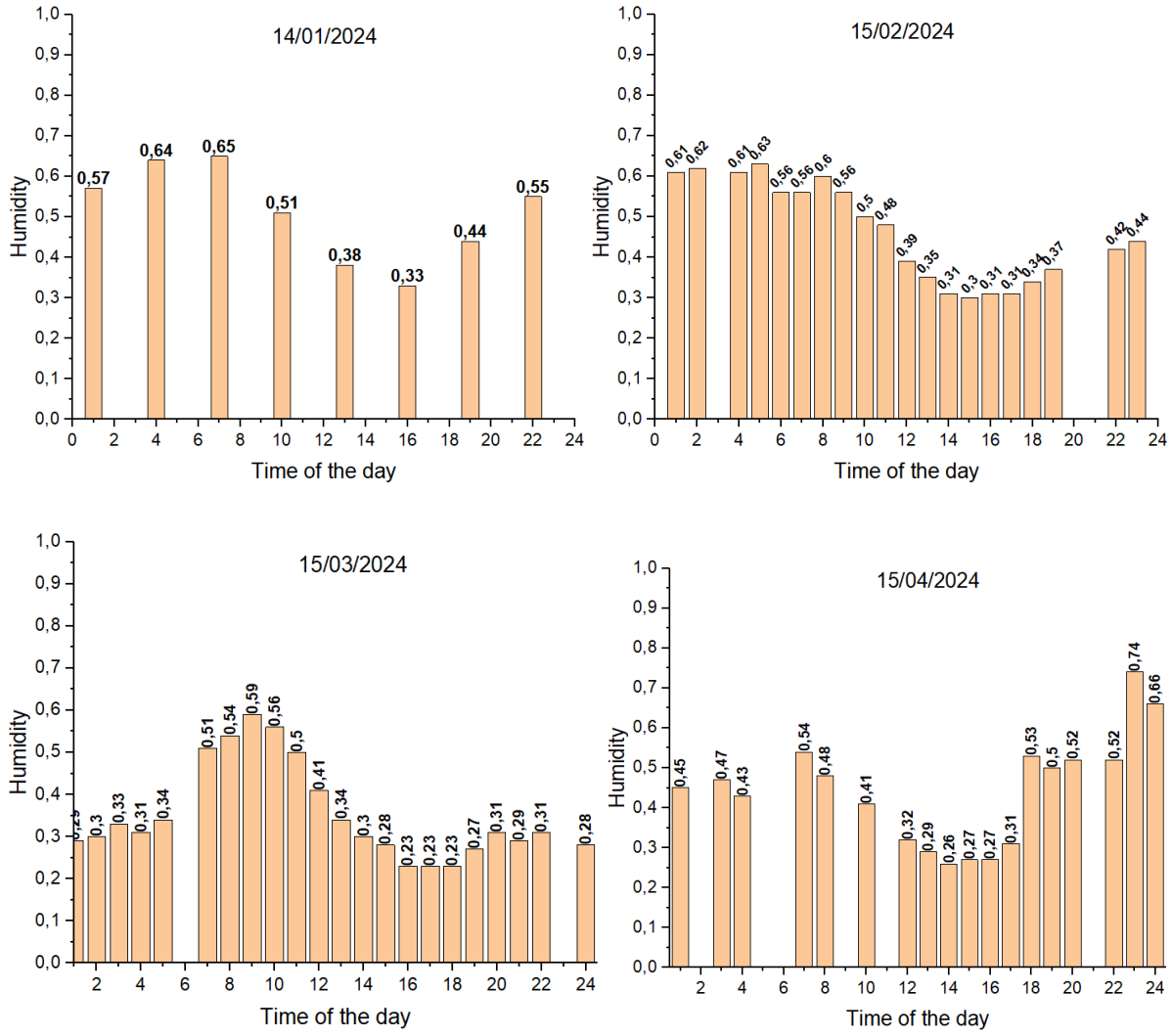

Fig.IV.2 Humidity versus of the time

The data extracted from the graphs show fluctuations in humidity levels at different times of the day for specific dates in the city of Biskra, see Fig IV.2. We can observe that there is an increase in humidity during the night and a relative decrease during the daytime between the

sunrise and sunset. The results show that the variation of humidity is versus the ambient temperature, see Fig IV.1. These results provide a deeper understanding of the weather conditions in the region and can assist in planning agricultural activities and other work affected by humidity levels.

IV.4 Wind speed of the site

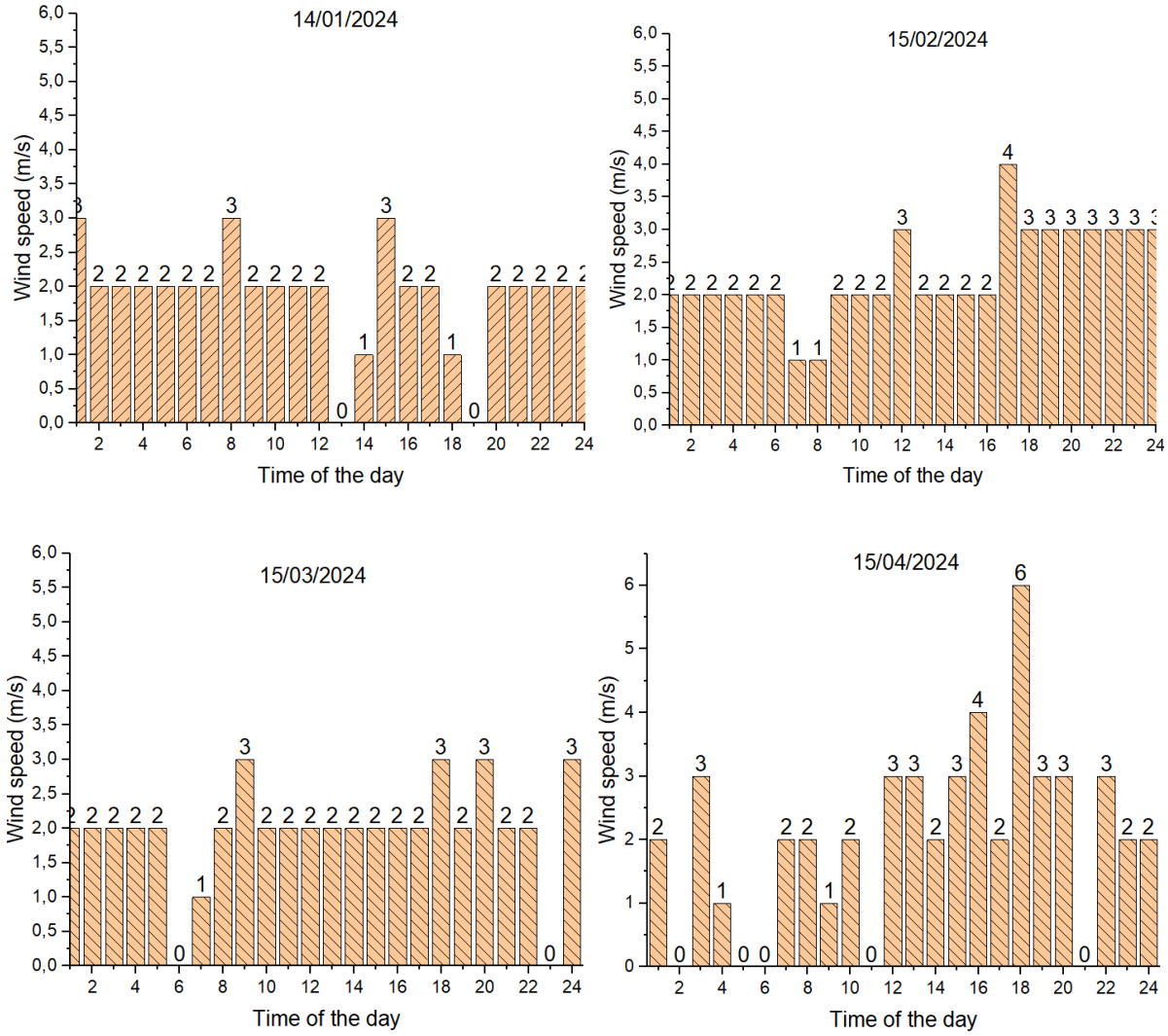

Fig .IV.3 Wind speed versus time of the day

Figure IV.3 shows the variation of the speed of wind as a function of the time of the day, based on the provided data we can be remarked that the wind speed in the city of Biskra changes throughout the day with irregular form is not stable. The graphs show that the highest recorded wind speed attains the value equal to 6 m/s on 15/05/2024 and sometimes with the lowest speed wind when it attains 0 m/s. These fluctuations indicate changes in weather conditions and can be indicative of climate variations or local natural phenomena

IV.5 Atmospheric pressure of the local

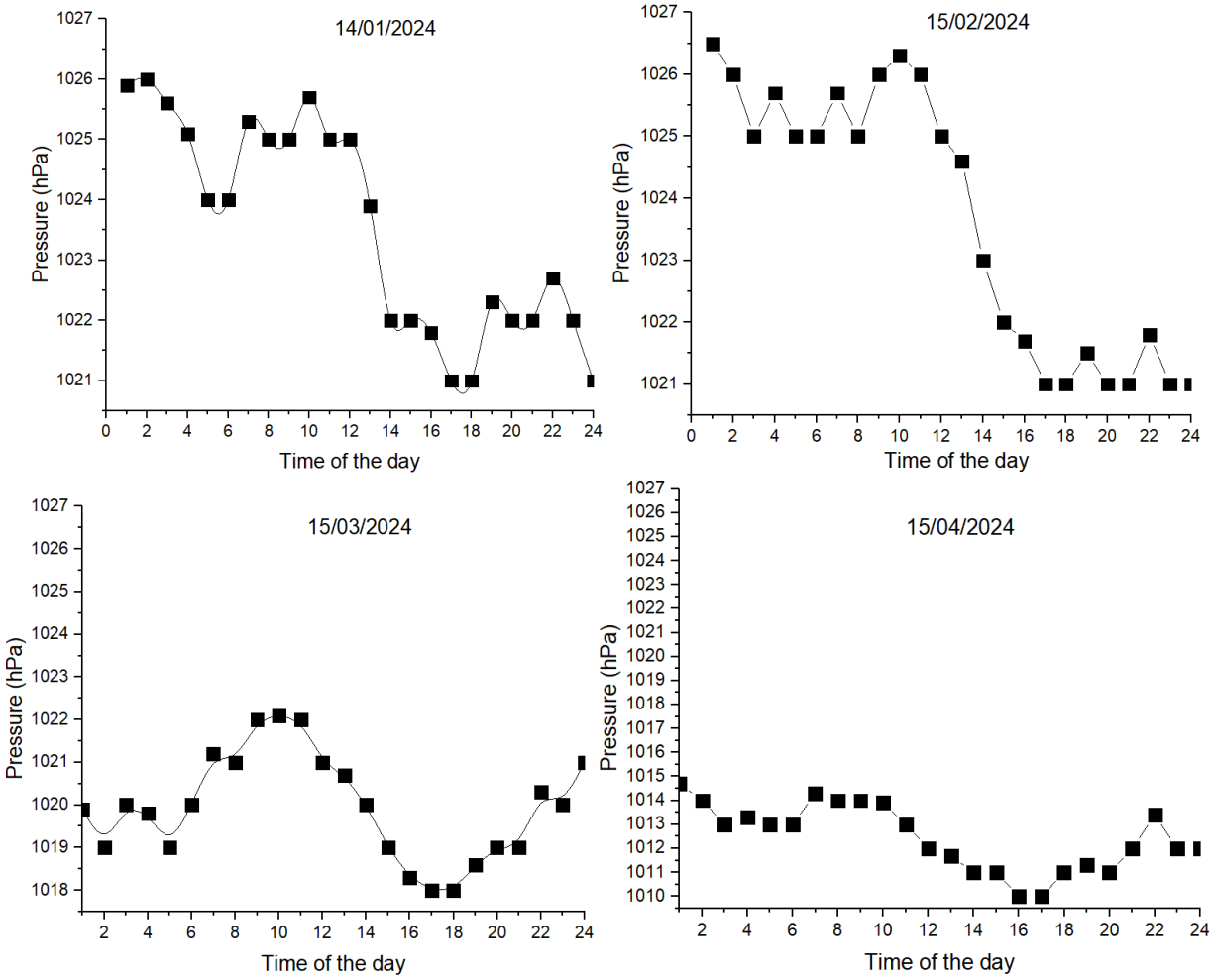

Fig.IV.4 Analysis of pressure versus the time

The graphs in Fig.IV.4 show the illustration of atmospheric pressure in Biskra over different days. There is a gradual decrease in atmospheric pressure between January and February, and then the fluctuation in the values of pressure in March and April means the seasonal changes or specific weather conditions. This data can be useful for weather forecasting and studying its effects on various human and natural activities in the region.

IV.6 Global solar radiation

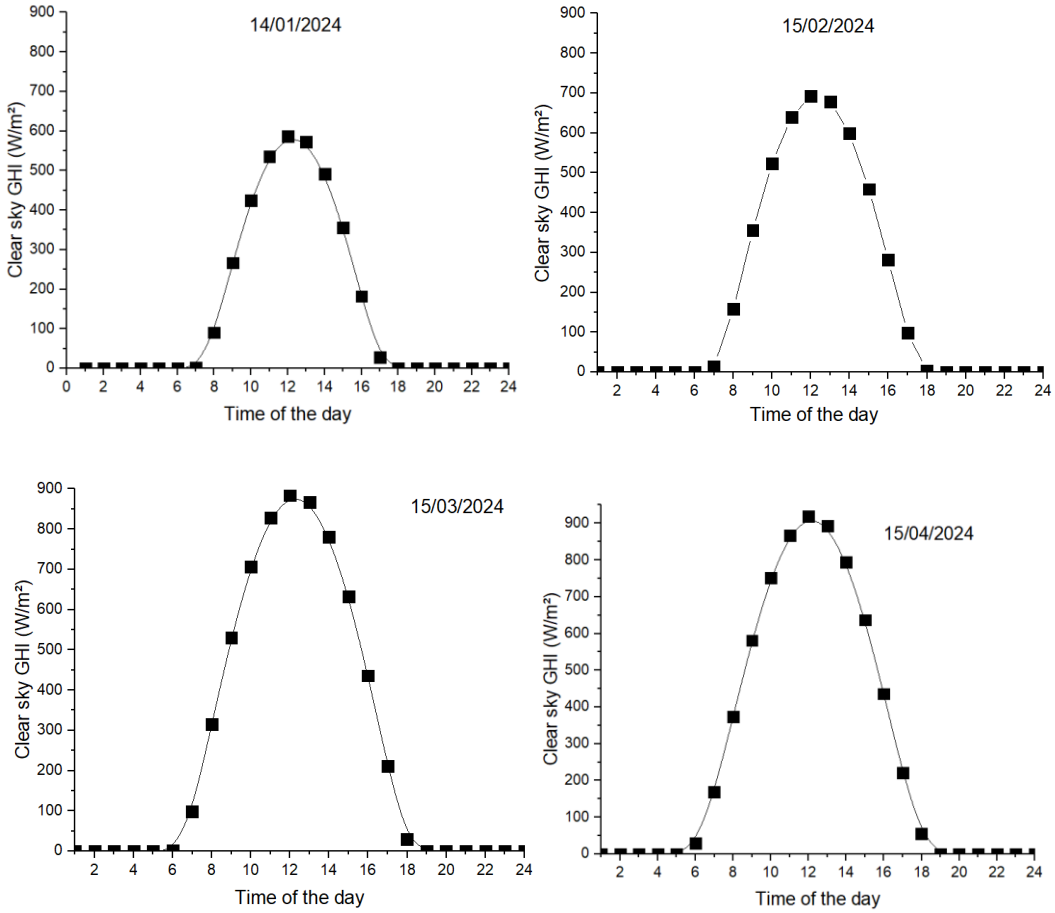

Fig.IV.5 Analysis of the global solar radiation depending on time

Figure IV.5 shows the variation of the global solar radiation as a function of time of the day according to four months of the year such as January, February, March, and April.

The analyzed global solar radiation data in Biskra shows a significant increase during midday hours, with peak values approaching between 700 and 900 (W/m²), according to the typical day. The global solar radiation selected low energy between sunrise and sunset, respectively of the beginning day with increase and finishing with decrease power, before and after sunshine, when the values of radiation attain zero, which means the sun is absent. The data reflects stable weather conditions and the availability of solar radiation across different days.

IV.7 Comparison of forecast and measurement of global solar radiation

Figure IV.6 represents the evolution as a function of the time of the day according to different months of the year, but we have selected the first four months such as January, February, March April. This part of the study shows the comparison between the forecast and measurement data, which indicates the best way of evolution of the global solar radiation with a perfect approach. Conclude that the mathematical model gives us the great evolution of global solar radiation which is a function of the different weather parameters such as ambient temperature, dew temperature, pressure, and height sun angle, all them controlled according to the number of months. This accuracy is observed over the four illustrated days. Noting the impact of geographical location and weather conditions on these values.

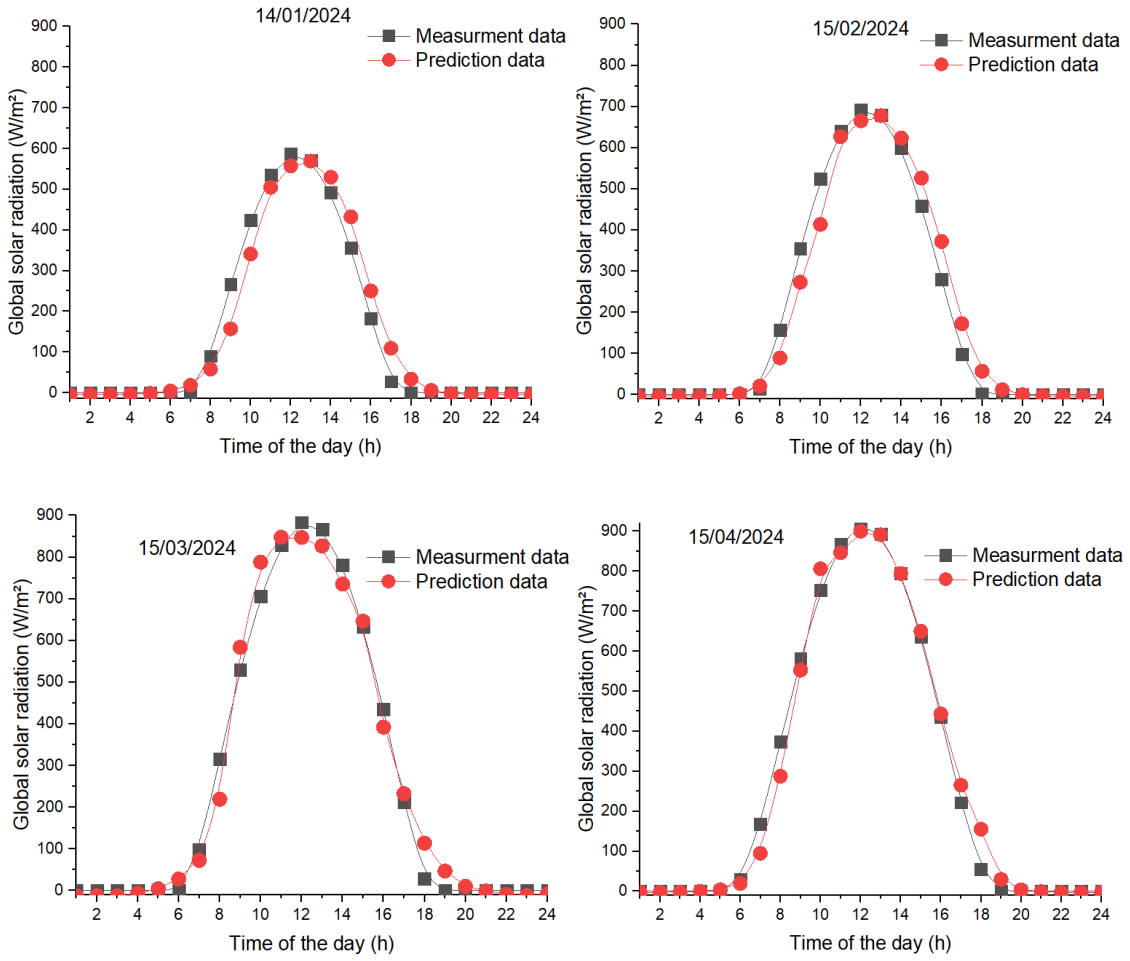

Fig .IV.6 Comparison of the prediction and measurement data of global solar radiation

IV.8 Illumination and global solar radiation versus time

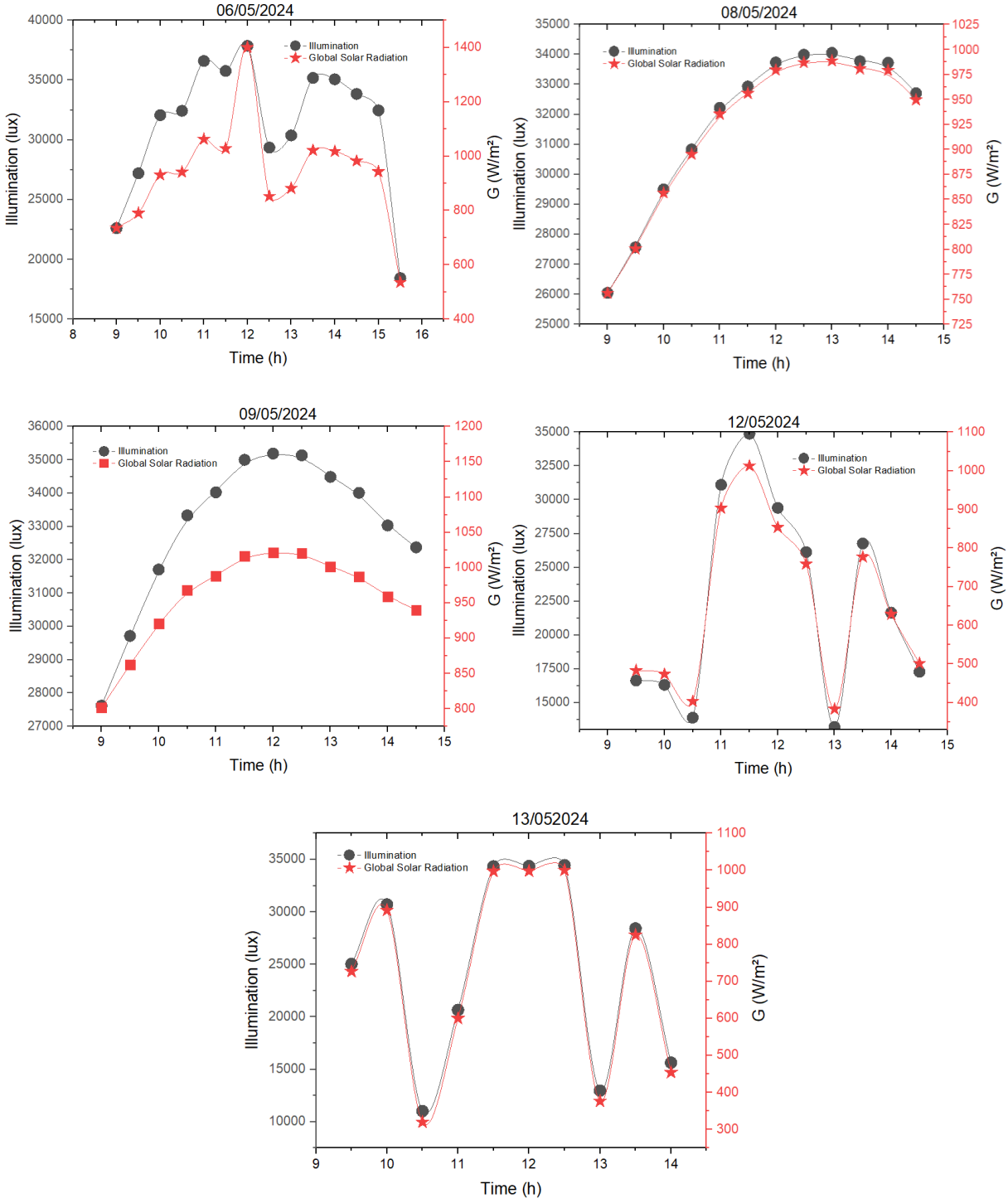

Fig. IV.7 Illumination and global solar radiation versus time corresponding to Arduino data

The illustration of the illumination and global solar radiation as a function to time the day of the tests, according to the same month with different days, see Fig.IV.7. This part of the result indicated the data of the Arduino system which installed next to hall technologic at University of Biskra. The illumination and the global radiation were measured by BH1750FVI

which was installed on the weather box. Conclude that evolution takes the same way between it. The Arduino helps us to know the surprise chock of the value between all parameters of the weather. These results indicate a direct effect of solar radiation on light intensity.

IV.9 Pressure and wind speed versus time

The wind is air pressure converted into movement of air. When air slows down, its pressure increases, see Fig.IV.8a and IV.8b. The kinetic energy or momentum of a moving air mass is converted into static atmospheric pressure as the air mass slows down. This means that higher wind speeds will show lower air pressure readings.

The analysis curves have indicated the relationship between atmospheric pressure and wind speed, where the wind speed increases directly the atmospheric pressure rises. The measurement data show the variation in atmospheric pressure decreases gradually against the wind speed as a function of the time of the day. Ultimately. the findings highlight the impact of atmospheric pressure on wind speed and the associated temporal changes.

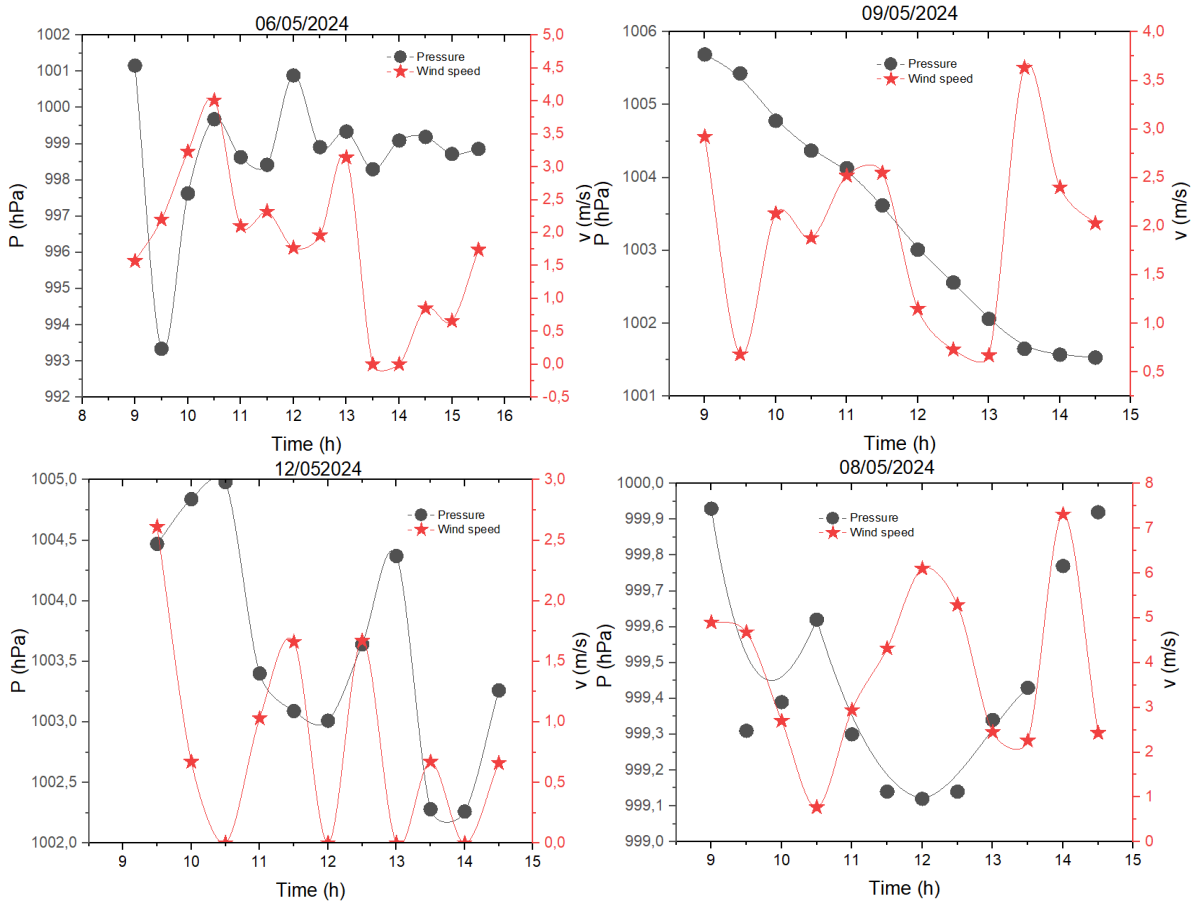

Fig.IV.8a Pressure and wind speed versus time

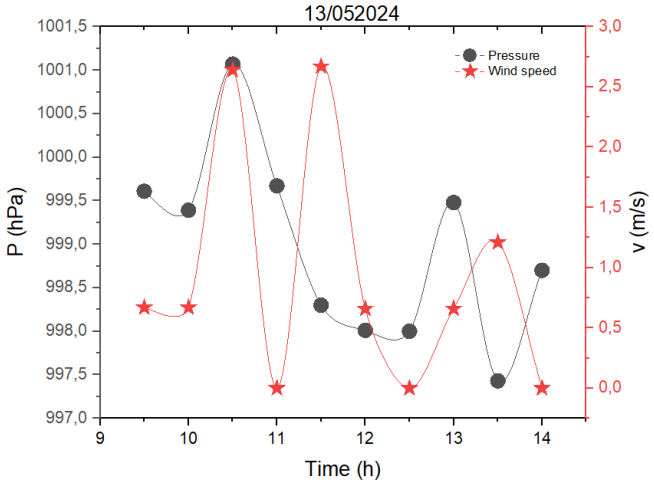

Fig.IV.8b Pressure and wind speed versus time

The analysis indicates a positive correlation between atmospheric pressure and wind speed. where wind speed increases as atmospheric pressure rises. The data also show a gradual decrease in atmospheric pressure and a gradual increase in wind speed over the indicated period. It is important to note that these results are based solely on the presented data and may be influenced by other external factors. Ultimately. the findings highlight the impact of atmospheric pressure on wind speed and the associated temporal changes.

IV. 10 Carbon dioxide and Ultraviolet versus time

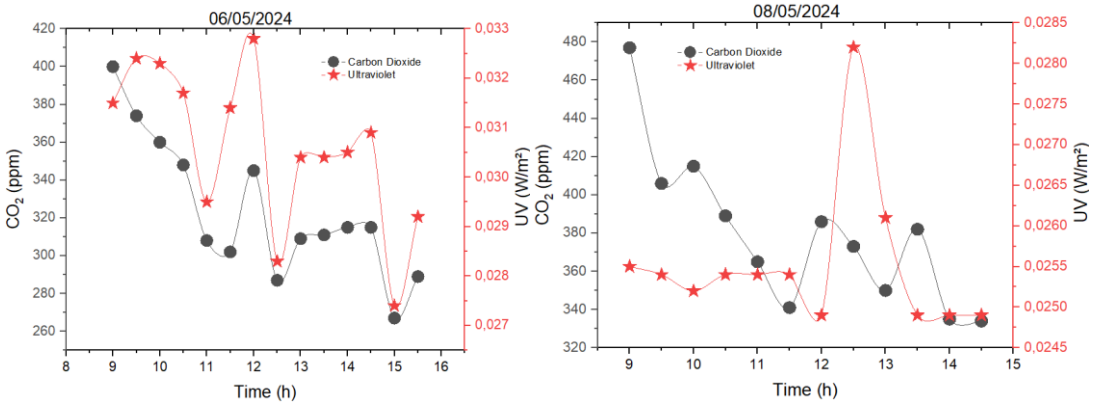

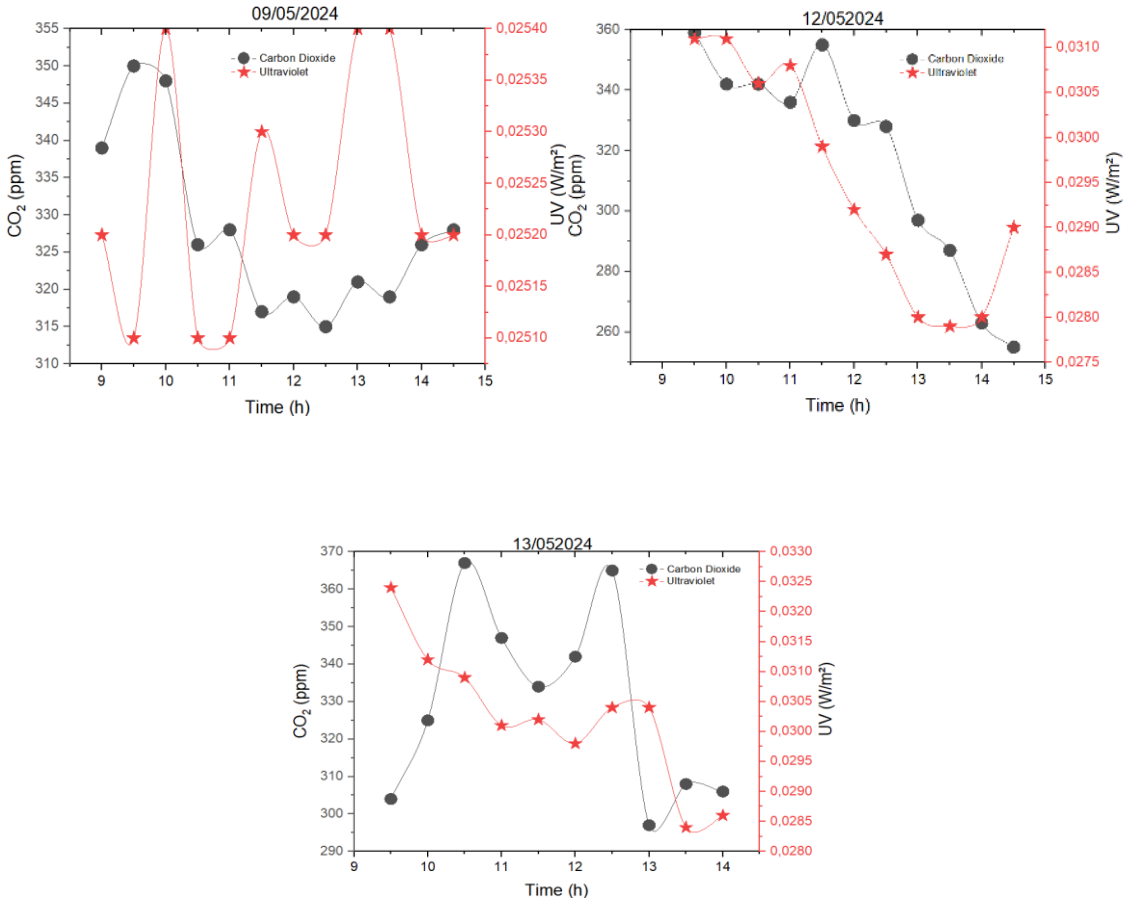

Fig.IV.9 Carbon dioxide and Ultraviolet versus time

Figure IV.9 represents the variation between the carbon dioxide and Ultraviolet as a function of the time of the day, corresponding to different days of the month. We have observed that the evolution the carbon dioxide is parallel with the variation the Ultraviolet, which sense has the same impact. The carbon dioxide took a maximum value attain to 480 ppm on 08/05/2024 the Ultraviolet constate 0.033 W/m² on 06/05/2024, and minimum value on 12/05/2024 by 255 ppm, and the Ultraviolet of 0.0251 W/m² at 09/05/2024.

IV.11 Ambient temperature and Humidity versus time

The curves show the variations in ambient temperature and relative humidity during the period from May 6th to May 13th. 2024, according to the time of the day, the results indicate that the ambient temperature started with a low value versus humidity taking high values. Observed that the ambient temperature has a maximum data in the day 06/05/2024 that variation explained in the figure IV.7 which show the variation of the global solar radiation attain to 1400 W/m².

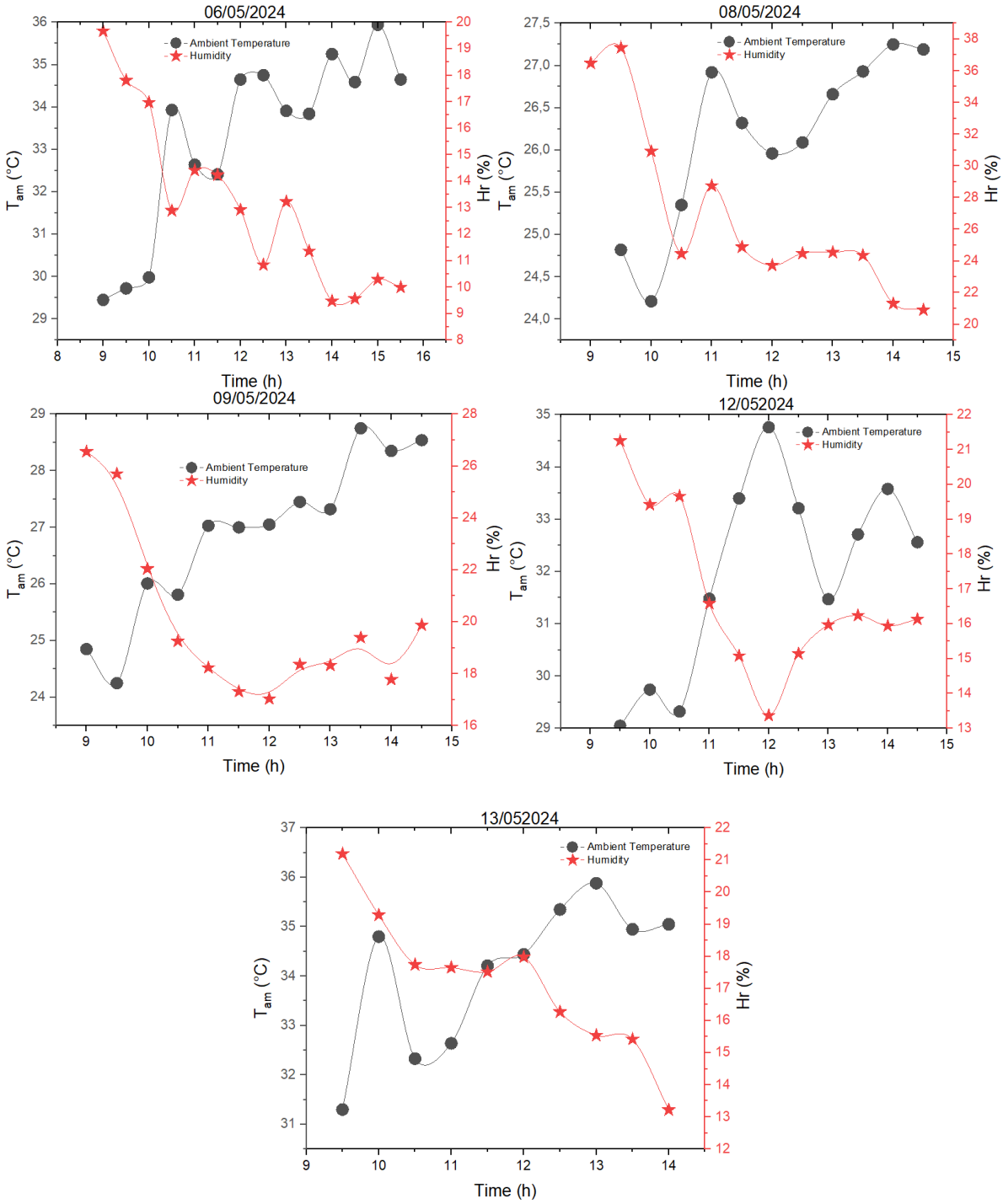

Fig.IV.10 Ambient temperature and Humidity versus time

IV.12 Conclusion

In this chapter, we have presented and analyzed the results of meteorological measurements, highlighting changes in ambient temperature, humidity, atmospheric pressure, wind speed, and global solar radiation. The analyses demonstrated the importance of precise measurements to understand the climatic changes and their practical applications, including the impact of global solar radiation on climate and the environment.

General conclusion

This memorandum represents a significant step towards a deeper understanding of the impact of meteorological variables on solar radiation and their utilization in developing accurate mathematical models. By analyzing variables such as temperature, humidity, and atmospheric pressure, and developing a mathematical model to predict solar radiation, we have provided a powerful tool to support climate studies and engineering applications.

The work was divided into two main parts: the first involved building the mathematical model using climatic data and analyzing it, and the second involved designing a measurement device based on the Arduino platform and various sensors to accurately measure atmospheric variables. Integrating this data into the mathematical model can offer more accurate predictions of solar radiation, helping to improve solar energy systems and enhance their efficiency.

During the experiments, the results showed a significant correlation between the mathematical model and the experimental data collected by the designed measurement device. This correlation confirms the model's effectiveness in simulating reality and providing accurate predictions of solar radiation based on the input meteorological variables. The ability to accurately predict solar radiation can contribute to better design and operation of solar energy systems, thereby promoting reliance on renewable energy.

We can say that this memorandum is not the end of the research but rather the beginning of broader and deeper applications. This model can be further developed to include more variables or to improve the accuracy of the sensors used. Additionally, the scope of the study can be expanded to cover different geographical areas, which will help enhance our understanding of the factors affecting solar radiation on a global scale.

, this work contributes to providing scientific and technological solutions to address environmental and energy challenges, laying a strong foundation for future projects that rely on real data and mathematical models to optimize the sustainable and efficient utilization of natural resources.

Bibliographic

[1]. Al-Ghezi. M. K. Mahmoud. B. K. Alnasser. T. & Chaichan. M. T. (2022). A Comparative Study of Regression Models and Meteorological Parameters to Estimate the Global Solar Radiation on a Horizontal Surface for Baghdad City. Iraq. International Journal of Renewable Energy Development. 11(1).

[2].Foued Chabane. Imene Laznek. Djamel Bensahal. (2018). Prediction of global solar radiation on the horizontal area with the effect of relative humidity part: I. ITALIAN JOURNAL OF ENGINEERING SCIENCE: TECNICA ITALIANA 61 2 pp: 115-118

[3]. Mefti. A.. Bouroubi. Y.. & Khellaf. A. (1999). Analyse critique du modèle de l'atlas solaire de l'Algérie. Journal of Renewable Energies. 2(2). 69-85.

[4]. Tadili. R.. & Bargach. M. N. (2005). Une méthode d'estimation du rayonnement solaire global reçu par une surface inclinée-Application aux sites marocains. La météorologie. 2005(50). 46-50.

[5]. Bouchouicha. K.. Hassan. M. A.. Bailek. N. & Aoun. N. (2019). Estimating the global solar irradiation and optimizing the error estimates under Algerian desert climate. Renewable energy. 139. 844-858.

[6]. Dahmani. A. Ammi. Y. & Hanini. S. Neural network for prediction solar radiation in Relizane region (Algeria)-Analysis study.

[7]. Besharat. F. Dehghan. A. A. & Faghih. A. R. (2013). Empirical models for estimating global solar radiation: A review and case study. Renewable and sustainable energy reviews. 21. 798-821.

[8]. Sabah. F. & SALMİ. M. (2021). Modeling of global solar radiation in Algeria based on geographical and all climatic parameters. International Journal of Computational and Experimental Science and Engineering. 7(3). 119-122.

[9]. Benatiallah. D. Benatiallah. A. Bouchouicha. K. & Nasri. B. (2020). Prediction du rayonnement solaire horaire En utilisant les reseaux de neurone artificiel. Algerian Journal of Environmental Science and Technology. 6(1).

[10]. Koussa. M. Malek. A. Haddadi. M. & Haddadi. E. M. (2007). Proposition d'une méthodologie de reconstitution des moyennes mensuelles par heure des irradiation diffuse et

globale en fonction des moyennes mensuelles par jour de quelques paramètres météorologiques. Rev. des Energies Renouvelables. Tlemcen. 255-68.

[11]. Chabane. F.. Ghedhifi. M. A.. Bensahal. D. Brima. A. & Moummi. N. (2018). Forecast of global solar irradiation with a perfect model according to incline angle. Journal of Power Technologies. 98(3). 245-254

[12]. Bayrakçı. H. C. Demircan. C. & Keçebaş. A. (2018). The development of empirical models for estimating global solar radiation on horizontal surface: A case study. Renewable and Sustainable Energy Reviews. 81. 2771-2782.

[13]. Chegaar. M. & Chibani. A. (1999). Methods for computing global solar radiation. Recueils des résumés des Journées Nationales pour la Valorisation des Energies Renouvelables. 23-24.

[14]. Yettou. F. Malek. A. Haddadi. M. & Gama. A. (2009). Etude comparative de deux modèles de calcul du rayonnement solaire par ciel clair en Algérie. Journal of Renewable Energies. 12(2). 331-346.

[15]. Mesri-Merad. M. Rougab. I. Cheknane. A.. & Bachari. N. E. I. (2012). Estimation du rayonnement solaire au sol par des modèles semi-empiriques. Journal of Renewable Energies. 15(3). 451-463.

[16] R. Imadeddine. A. Yassine. « Etude et réalisation d'une station météo connectée par

Wifi ». Mémoire de master. université MOHAMED BOUDIAF – M'SILA2017.

[17] https://forum.arduino.cc/t/arduino-mega2560-r3-pinouts-photo/123330

[18] https://www.carnetdumaker.net/articles/utiliser-un-capteur-de-temperature-et-

Dhumidite-dht11- .Mise à jour Avril 2021.

[19] http://electroniqueamateur.blogspot.com/2016/06/mesurer-la-pression-atmospherique-

[20] https://www.vernier.com/manuals/sms-bta/

[21] https://robocraze.com/products/mq-135-gas-sensor-module

[22] https://hobbycomponents.com/sensors/389-25v-voltage-sensor-module

[23] https://yadom.eu/grove-capteur-uv.html

[24] https://www.robotics.org.za/MICRO-SD-SIL

[25] https://zestedesavoir.com/tutoriels/686/arduino-premiers-pas-en-informatique-Embarquee/742_decouverte-de-larduino/3416_le-logiciel

[26] https://elektronicavoorjou.nl/fr/langage-de-programmation-arduino

[27] https://projecthub.arduino.cc/arcaegecengiz/using-dht11-12f621

[28] https://projecthub.arduino.cc/Aswinth/soil-moisture-sensor-with-arduino-91c818

[29]https://www.hackster.io/sheekar/mq-135-sensor-co2-benzyne-with-arduino-sheekar-banerjee-ab6ccd

[30] https://robojax.com/learn/arduino/?vid=robojax-BMP180

[31] https://robojax.com/learn/arduino/?vid=robojax_BH1750_light_lux_sensor

[32] https://pimylifeup.com/arduino-uv-sensor-veml6075/

[33]. https://www.infoclimat.fr/observations-meteo/archives/5/mai/2024/biskra/60525.html